

Neue Wege in der CT-Bildrekonstruktion



Marc Kachelrieß

German Cancer Research Center (DKFZ)

Heidelberg, Germany

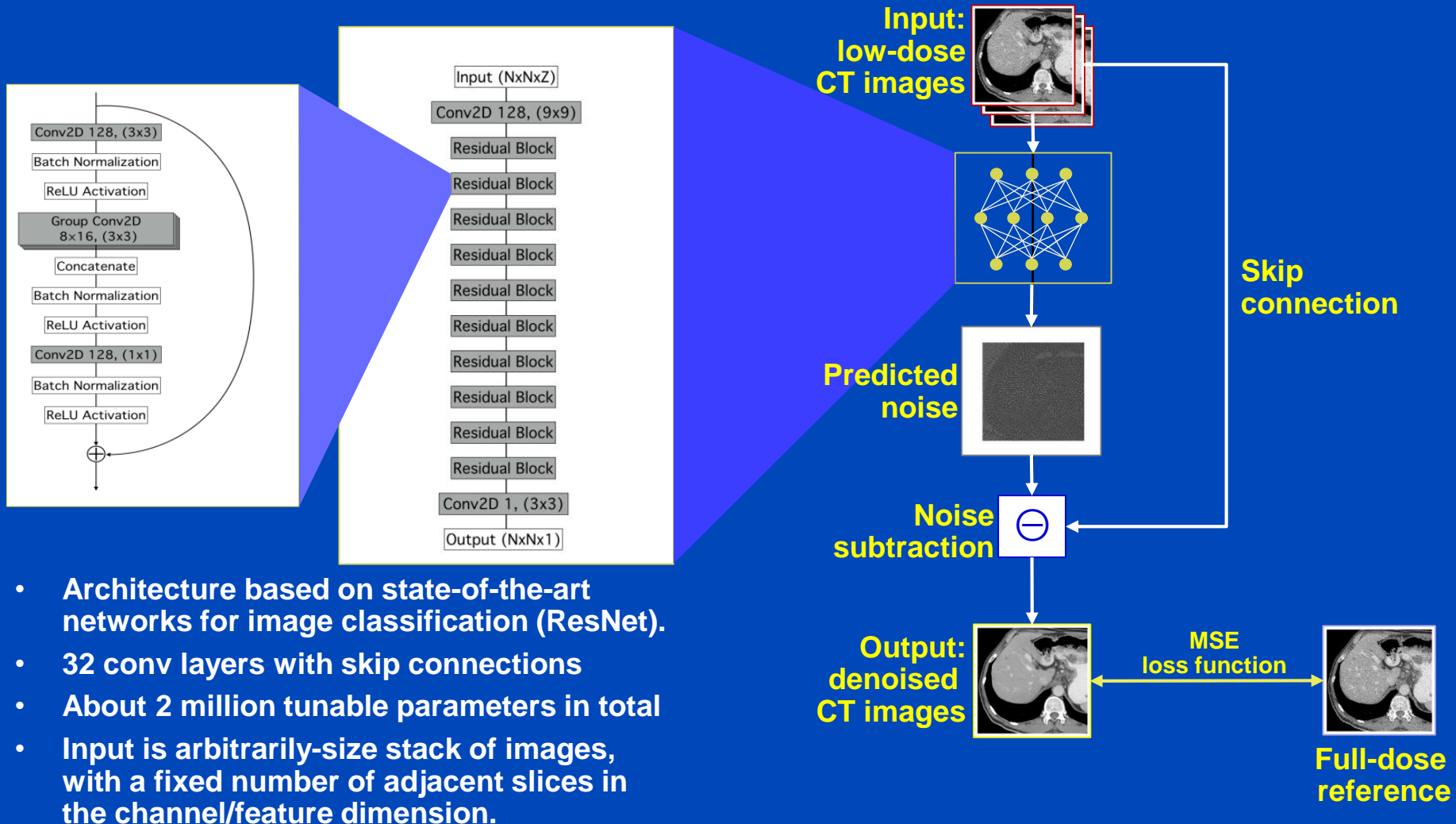
www.dkfz.de/ct

Content

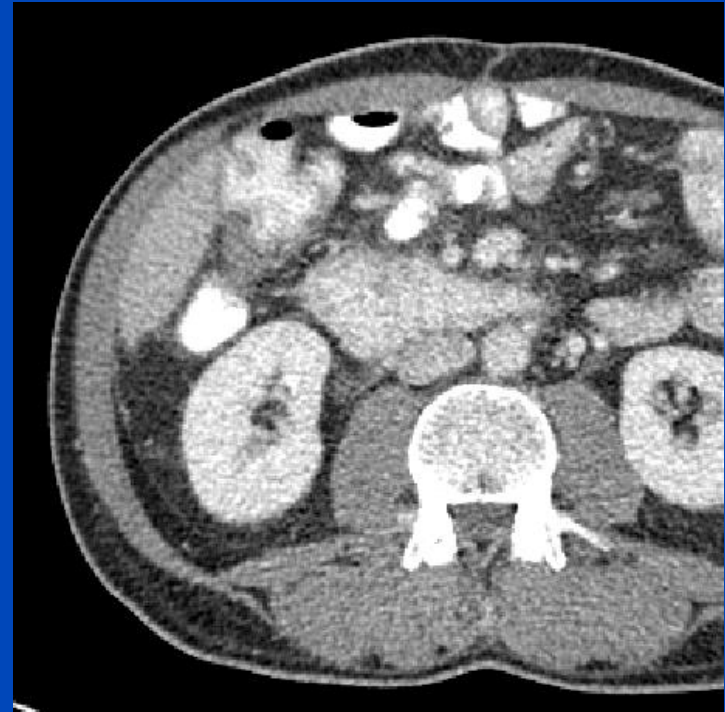
- **Noise reduction**
- **True and fake DECT**
- **Scatter estimation**
- **Dose estimation**
- **Motion compensation**
- **Not shown**
 - **Metal artifact reduction**
 - **Ring artifact removal**
 - **Limited angle reconstruction**
 - **Resolution enhancement**
 -

Noise Reduction

Noise Removal

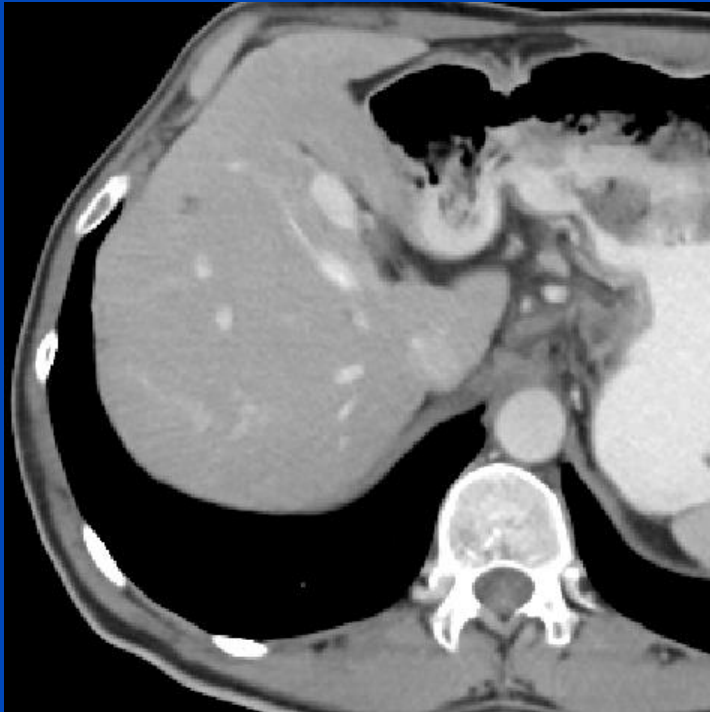


Noise Removal



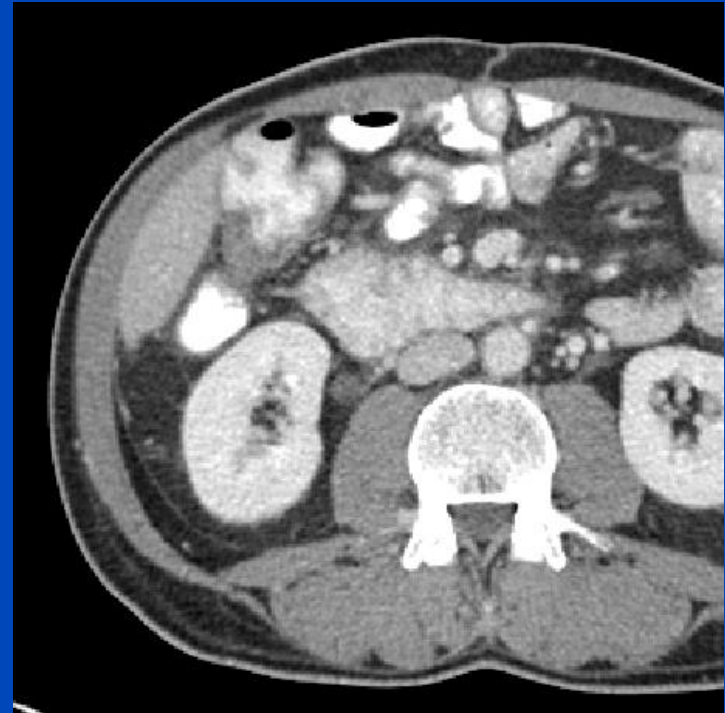
Low dose images (1/4 of full dose)

Noise Removal



Denoised low dose

Noise Removal



Full dose

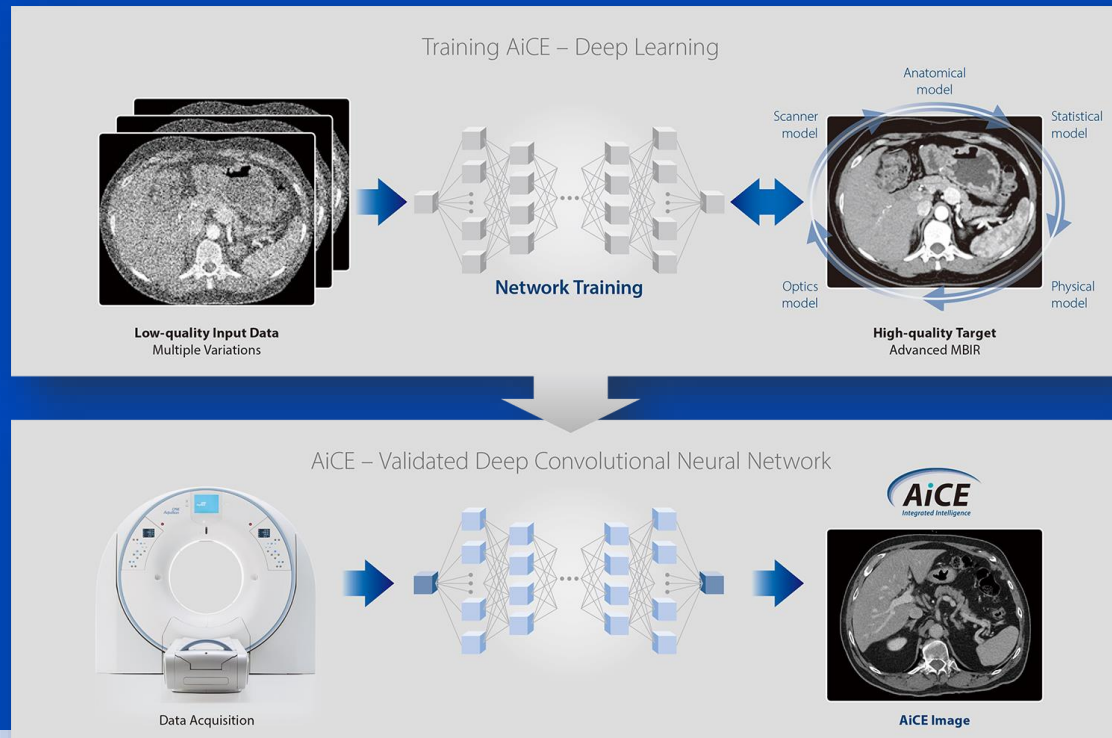
Noise Removal



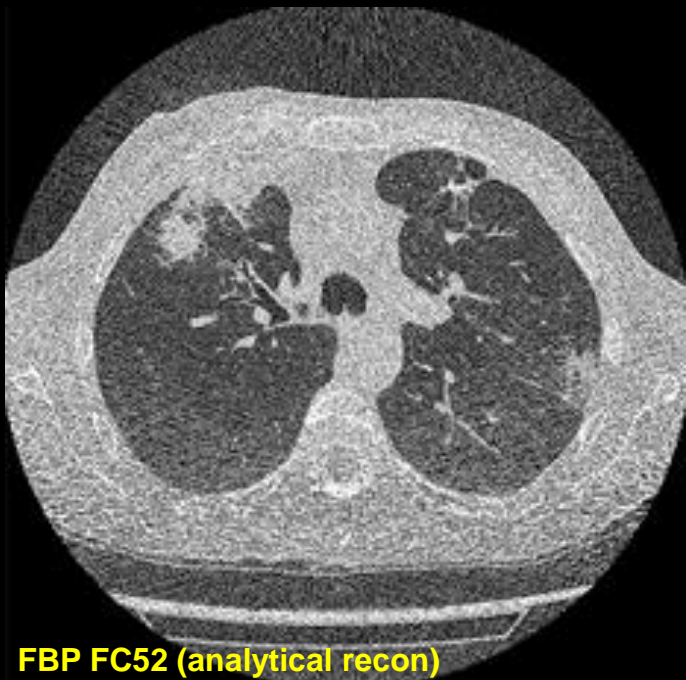
Denoised full dose

Canon's AiCE

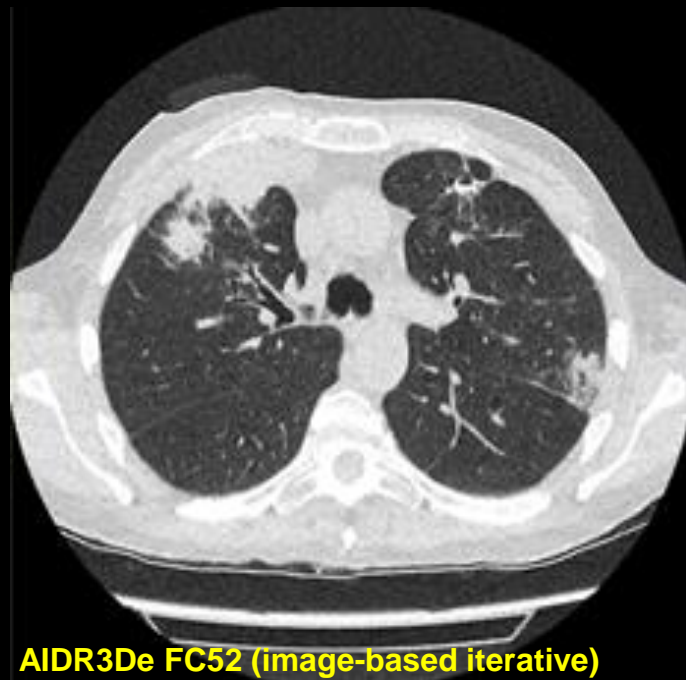
- Advanced intelligent Clear-IQ Engine (AiCE)
- Trained to restore low-dose CT data to match the properties of FIRST, the model-based IR of Canon.
- FIRST is applied to high-dose CT images to obtain a high fidelity training target



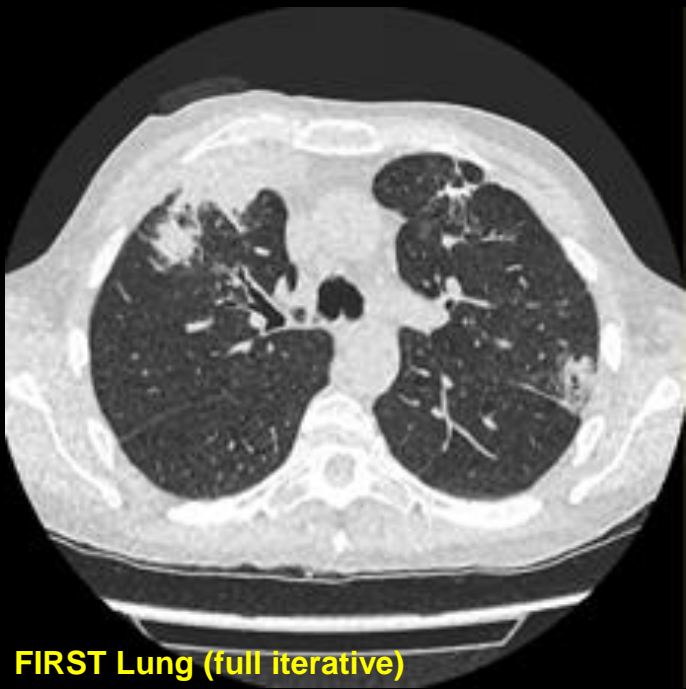
U = 100 kV
CTDI = 0.6 mGy
DLP = 24.7 mGy·cm
D_{eff} = 0.35 mSv



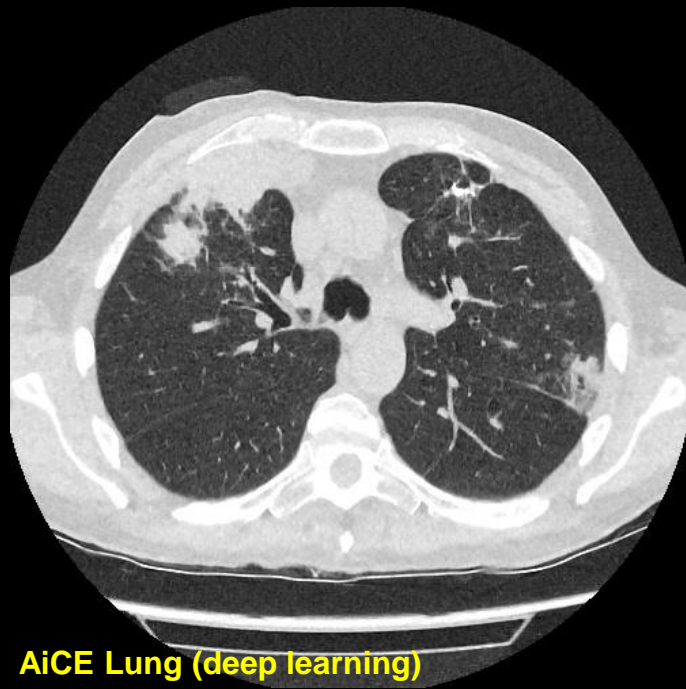
FBP FC52 (analytical recon)



AIDR3De FC52 (image-based iterative)

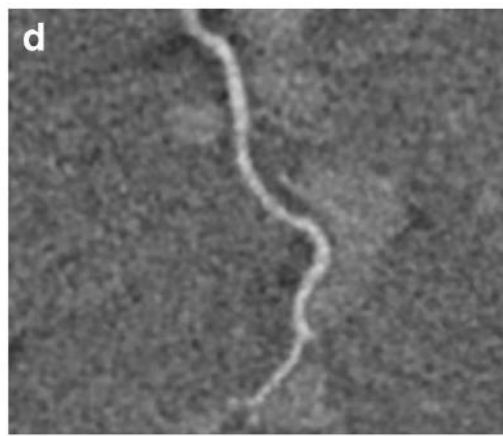
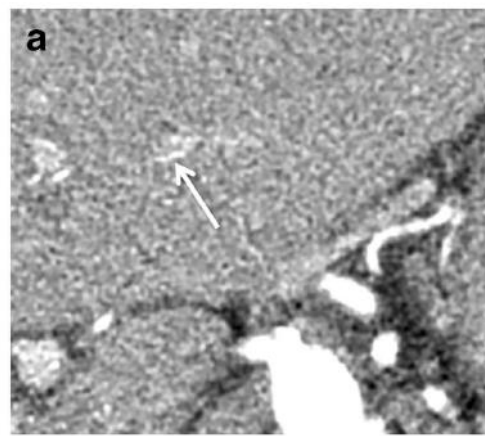


FIRST Lung (full iterative)

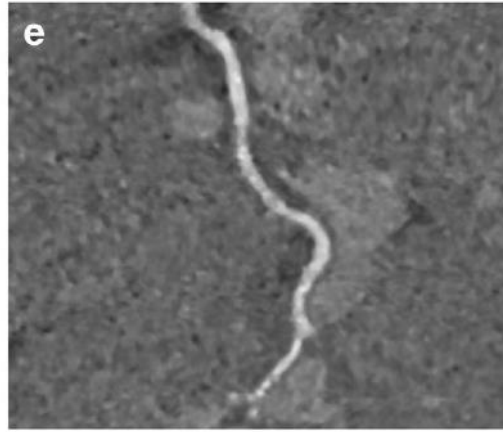
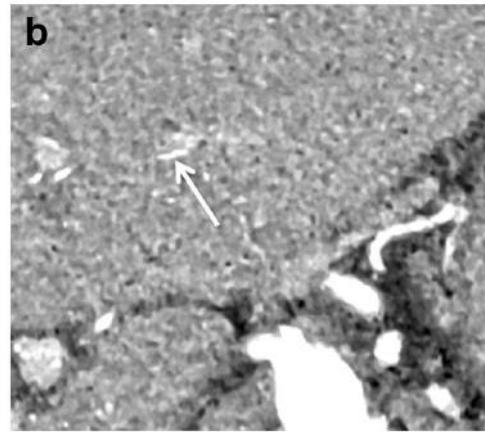


AiCE Lung (deep learning)

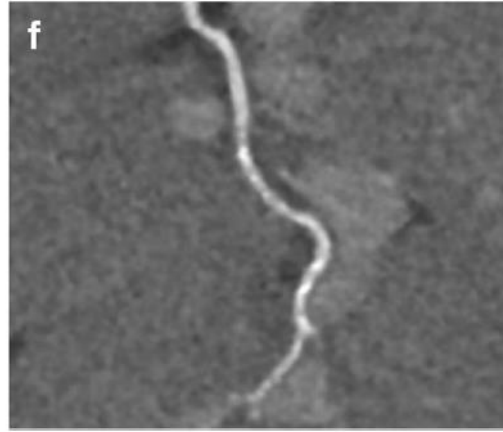
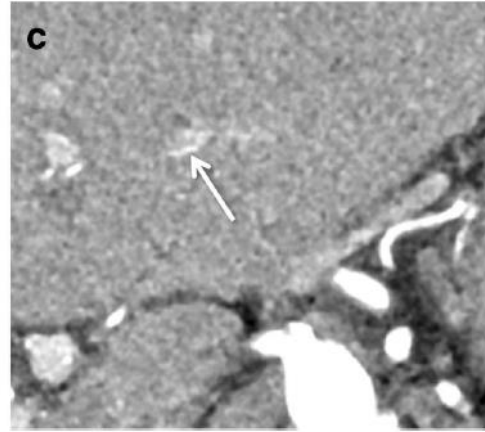
AIDR 3D



First



AiCE



GE's True Fidelity

- Based on a deep CNN
- Trained to restore low-dose CT data to match the properties of Veo, the model-based IR of GE.
- No information can be obtained in how the training is conducted for the product implementation.

2.5D DEEP LEARNING FOR CT IMAGE RECONSTRUCTION USING A MULTI-GPU IMPLEMENTATION

Amirkoushyar Ziabari*, Dong Hye Ye * †, Somesh Srivastava ‡, Ken D. Sauer ⊕
Jean-Baptiste Thibault ‡, Charles A. Bouman*

* Electrical and Computer Engineering at Purdue University

† Electrical and Computer Engineering at Marquett University

‡ GE Healthcare

⊕ Electrical Engineering at University of Notre Dame

ABSTRACT

While Model Based Iterative Reconstruction (MBIR) of CT scans has been shown to have better image quality than Filtered Back Projection (FBP), its use has been limited by its high computational cost. More recently, deep convolutional neural networks (CNN) have shown great promise in both denoising and reconstruction applications. In this research, we propose a fast reconstruction algorithm, which we call Deep Learning MBIR (DL-MBIR).

streaking artifacts caused by sparse projection views in CT images [8]. More recently, Ye, et al. [9] developed method for incorporating CNN denoisers into MBIR reconstruction as advanced prior models using the Plug-and-Play framework [10, 11].

In this paper, we propose a fast reconstruction algorithm, which we call Deep Learning MBIR (DL-MBIR), for approximately achieving the improved quality of MBIR using a deep residual neural network. The DL-MBIR method is trained to



FBP



ASIR V 50%



True Fidelity

Courtesy of GE Healthcare

True and Fake DECT

Existing fake DECT approaches (as of May 2022):

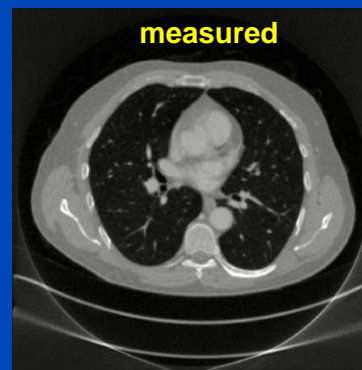
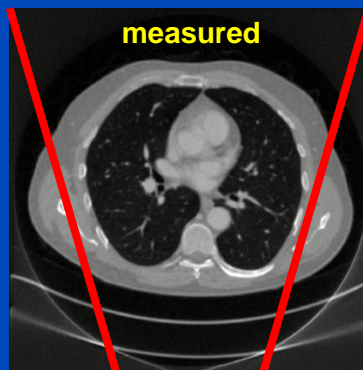
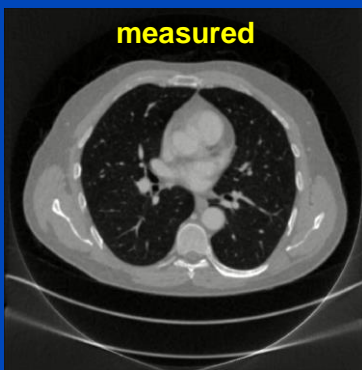
- [1] J. Ma, Y. Liao, Y. Wang, S. Li, J. He, D. Zeng, Z. Bian, “**Pseudo dual energy CT** imaging using deep learning-based framework: basic material estimation“, *SPIE Medical Imaging 2018*.
- [2] W. Zhao, T. Lv, P. Gao, L. Shen, X. Dai, K. Cheng, M. Jia, Y. Chen, L. Xing, “A deep learning approach for dual-energy CT imaging **using a single-energy CT** data”, *Fully3D 2019*.
- [3] D. Lee, H. Kim, B. Choi, H. J. Kim, “Development of a deep neural network for generating synthetic dual-energy chest x-ray images **with single x-ray exposure**”, *PMB 64(11)*, 2019.
- [4] L. Yao, S. Li, D. Li, M. Zhu, Q. Gao, S. Zhang, Z. Bian, J. Huang, D. Zeng, J. Ma, “Leveraging deep generative model for direct energy-resolving CT imaging **via existing energy-integrating CT** images”, *SPIE Medical Imaging 2020*.
- [5] D. P. Clark, F. R. Schwartz, D. Marin, J. C. Ramirez-Giraldo, C. T. Badea, “Deep learning based **spectral extrapolation** for dual-source, dual-energy x-ray CT”, *Med. Phys.* 47 (9): 4150–4163, 2020.
- [6] C. K. Liu, C. C. Liu, C. H. Yang, H. M. Huang, “Generation of brain dual-energy CT **from single-energy CT** using deep learning”, *Journal of Digital Imaging* 34(1):149–161, 2021.
- [7] T. Lyu, W. Zhao, Y. Zhu, Z. Wu, Y. Zhang, Y. Chen, L. Luo, S. Li, L. Xing, “Estimating dual-energy CT imaging **from single-energy CT** data with material decomposition convolutional neural network”, *Medical Image Analysis* 70:1–10, 2021.
- [8] F. R. Schwartz, D. P. Clark, Y. Ding, J. C. Ramirez-Giraldo, C. T. Badea, D. Marin, “Evaluating renal lesions using **deep-learning based extension** of dual-energy FoV in dual-source CT—A retrospective pilot study”, *European Journal of Radiology* 139:109734, 2021.
- [9] Y. Li, X. Tie, K. Li, J. W. Garrett, G.-H. Chen, “Deep-En-Chroma: **mining the spectral fingerprints in single-kV CT** acquisitions using energy integration detectors”, *SPIE Medical Imaging 2022*.

**Real DECT
(ground truth)**

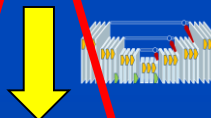
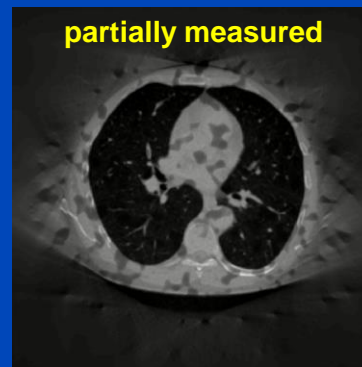
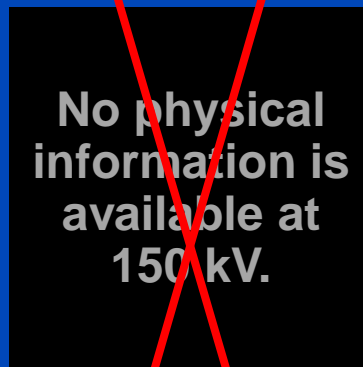
**Fake DECT
(often proposed)**

**Partial DECT
(small B FOM)**

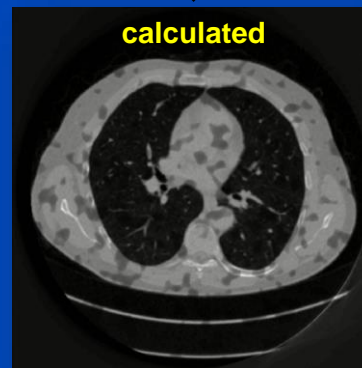
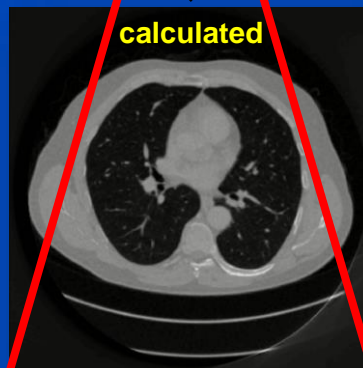
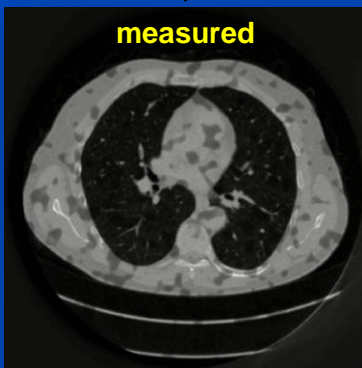
70 kV



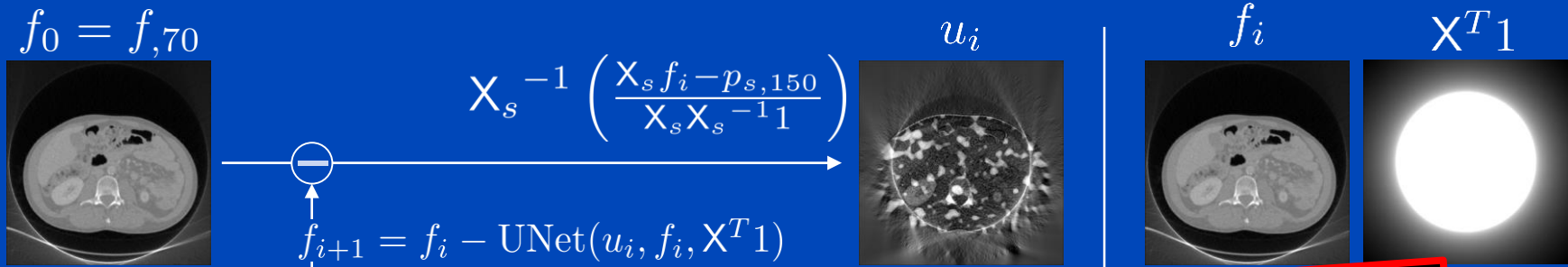
150 kV Sn



final 150 kV Sn

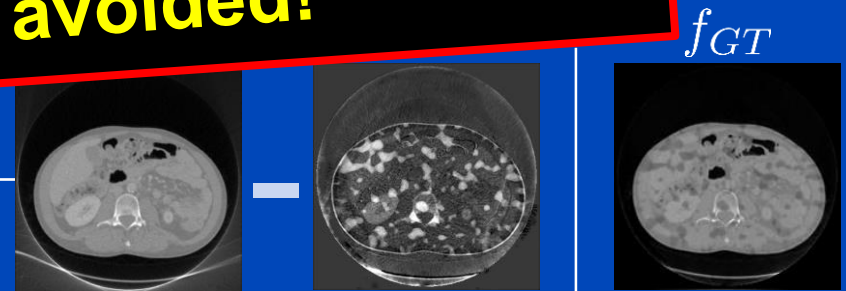


Algorithm for Partial DECT



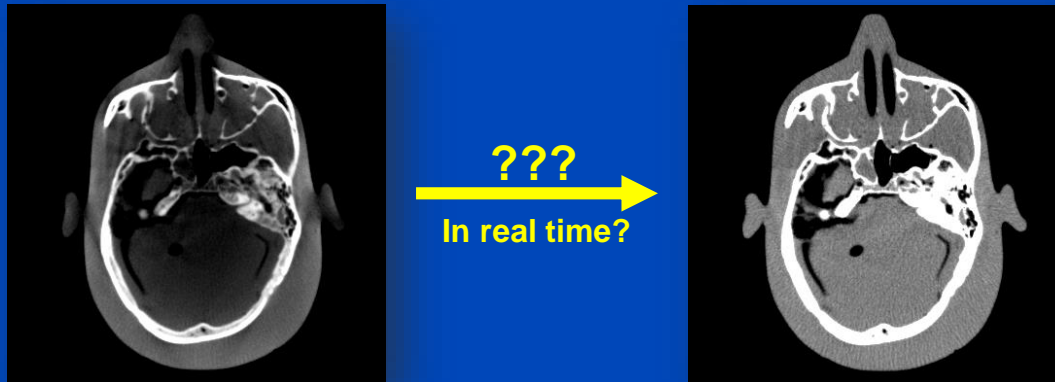
Conclusion:

Measuring the physical properties of the patient at more than one energy cannot be avoided!



$$L = \|w \cdot (f_i - \text{UNet}_i(u_i, f_i, X^T 1) - f_{GT})\|^2$$

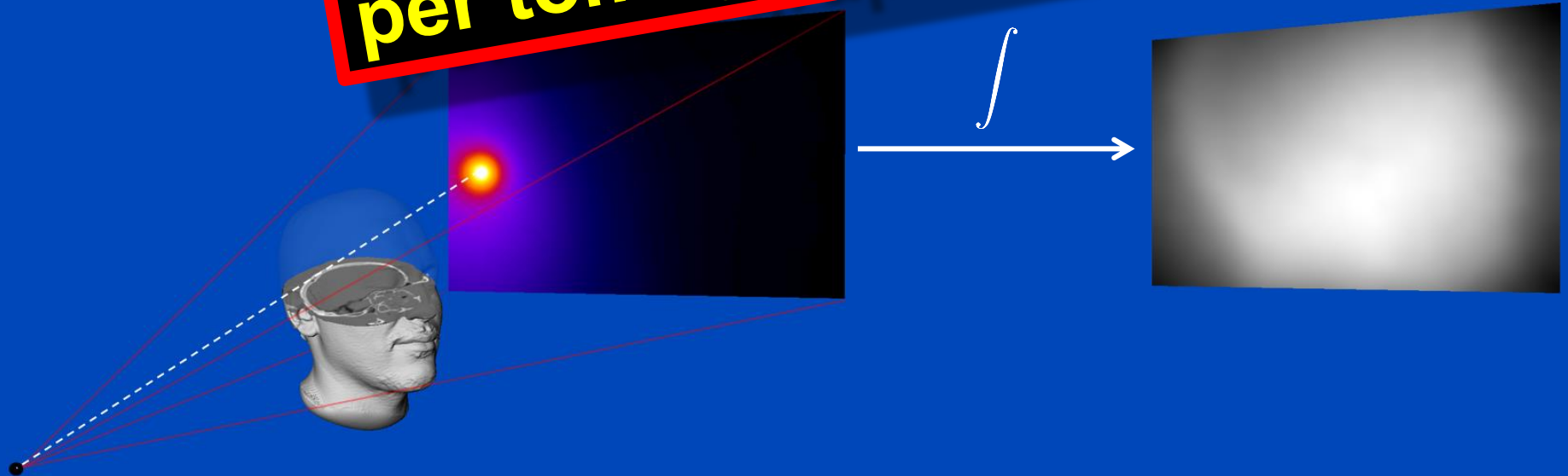
Deep Scatter Estimation



Monte Carlo Scatter Estimation

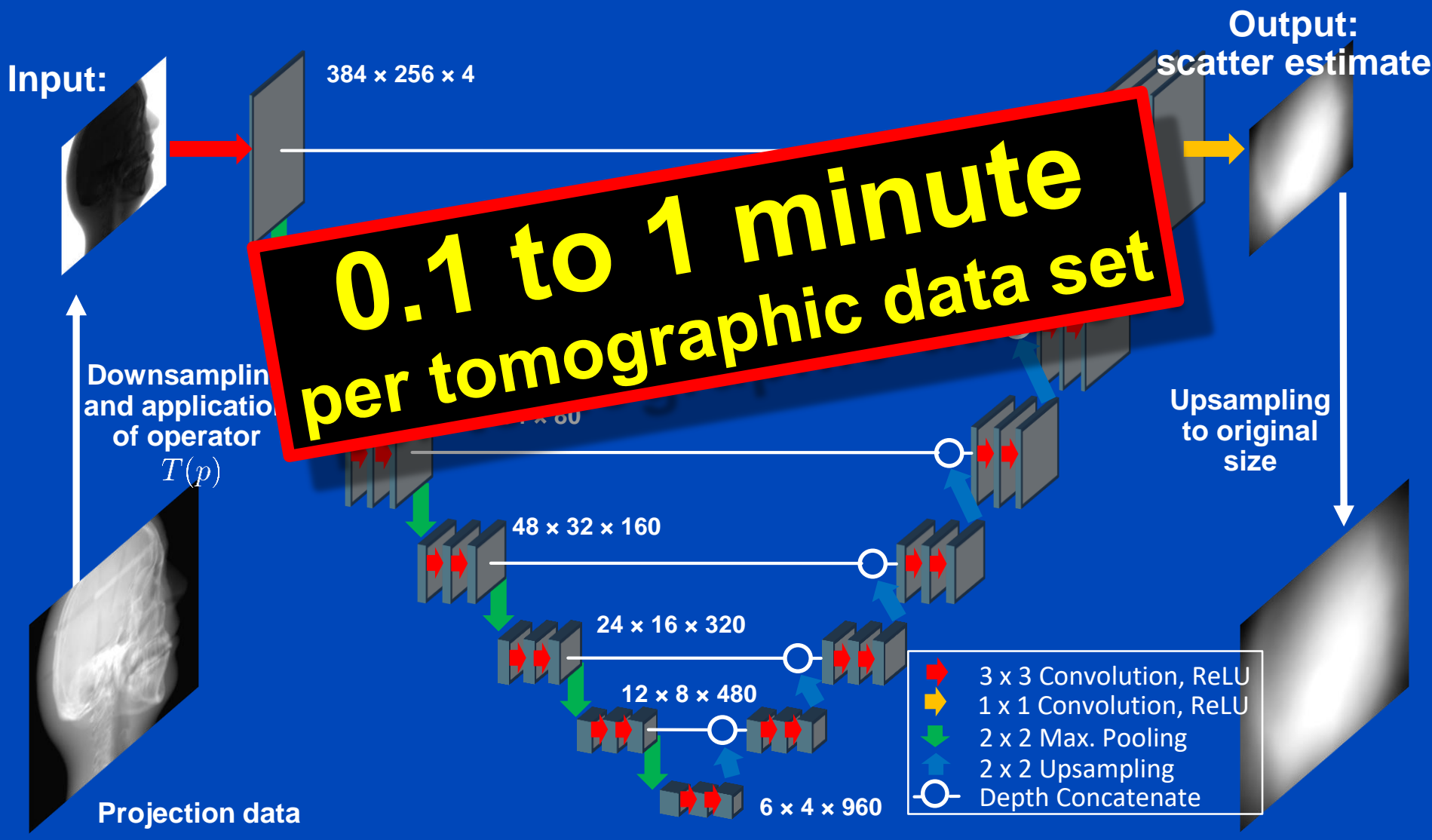
- Simulation of photon trajectories according to physical interaction probabilities.
- Simulating a large number of trajectories well approximates the complete scatter distribution

**1 to 10 hours
per tomographic data set**



Deep Scatter Estimation

Network architecture & scatter estimation framework



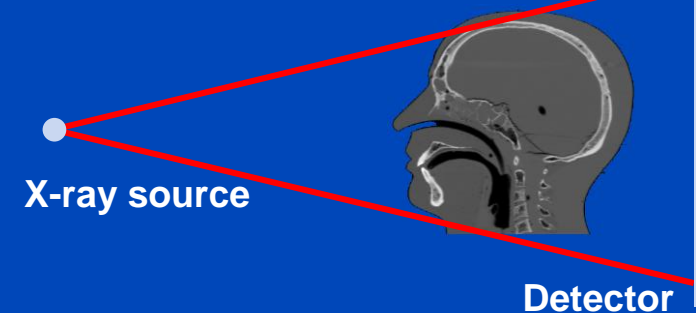
Testing of the DSE Network for Measured Data (120 kV)

DKFZ table-top CT

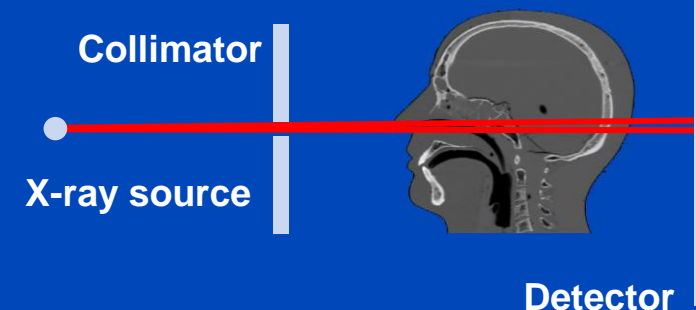


- Measurement of a head phantom at our in-house table-top CT.
- Slit scan measurement serves as ground truth.

Measurement to be corrected



Ground truth: slit scan



Reconstructions of Measured Data

Slit Scan

No Correction

Kernel-Based
Scatter Estimation

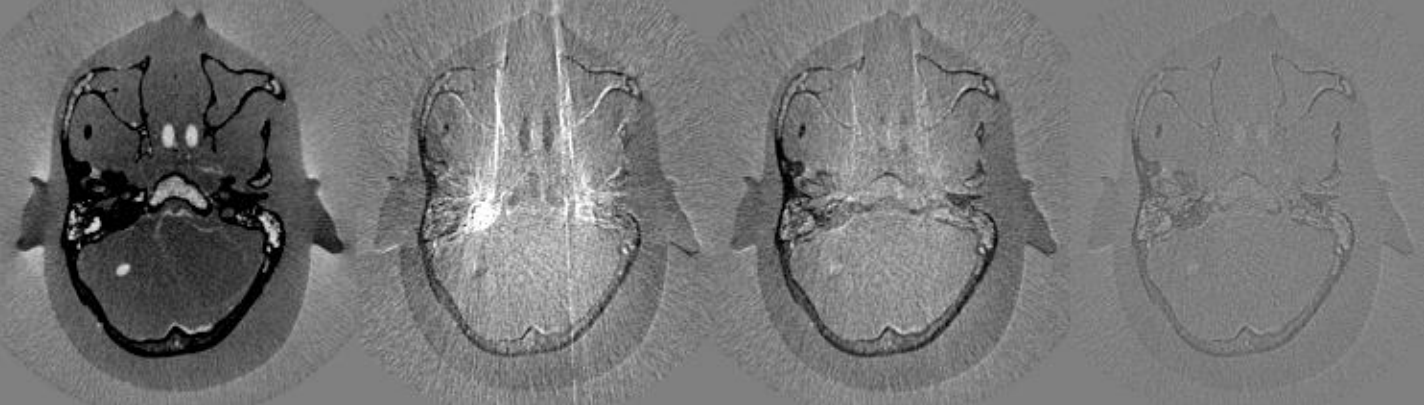
Hybrid Scatter
Estimation

Deep Scatter
Estimation

CT Reconstruction



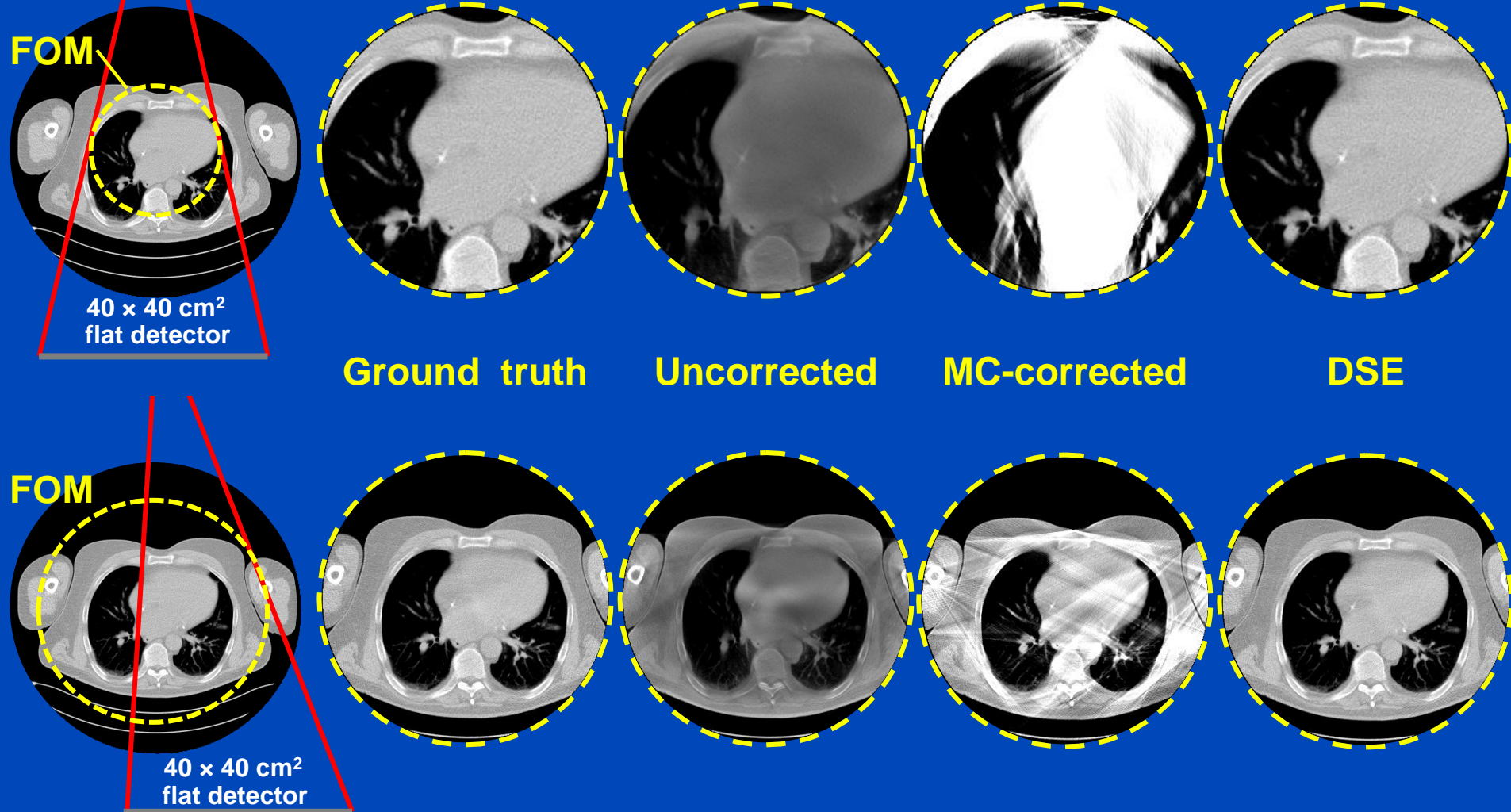
Difference to slit scan



$C = 0 \text{ HU}, W = 1000 \text{ HU}$

A simple detruncation was applied to the rawdata before reconstruction. Images were clipped to the FOM before display. $C = -200$ HU, $W = 1000$ HU.

Truncated DSE^{1,2}



To learn why MC fails at truncated data and what significant efforts are necessary to cope with that situation see [Kachelrieß et al. Effect of detruncation on the accuracy of MC-based scatter estimation in truncated CBCT. Med. Phys. 45(8):3574-3590, August 2018].

¹J. Maier, M. Kachelrieß et al. Deep scatter estimation (DSE) for truncated cone-beam CT (CBCT). RSNA 2018.

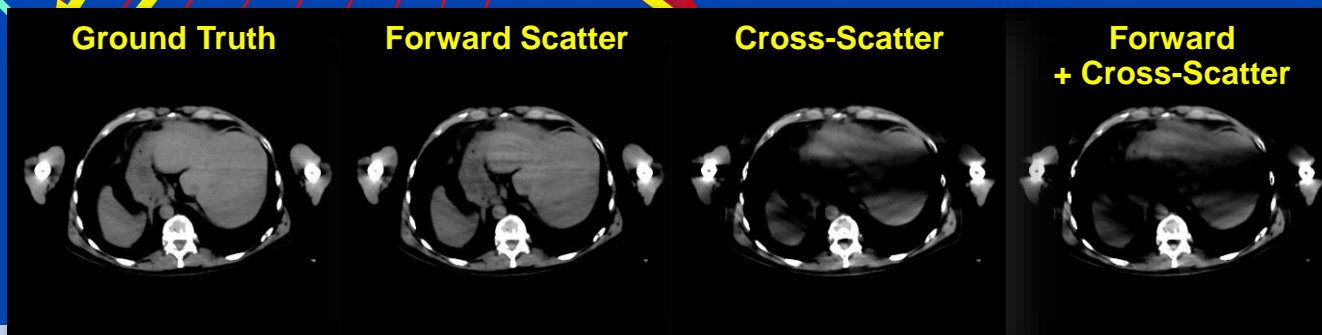
²J. Maier, M. Kachelrieß et al. Robustness of DSE. Med. Phys. 46(1):238-249, January 2019.

Scatter in Dual Source CT (DSCT)



Siemens SOMATOM Force
dual source cone-beam spiral CT

$$q = -\ln \frac{I_{\text{primary}} + S_{\text{forward}} + \rho S_{\text{cross}}}{I_0}$$



C = 40 HU, W = 300 HU, with 2D anti-scatter grid

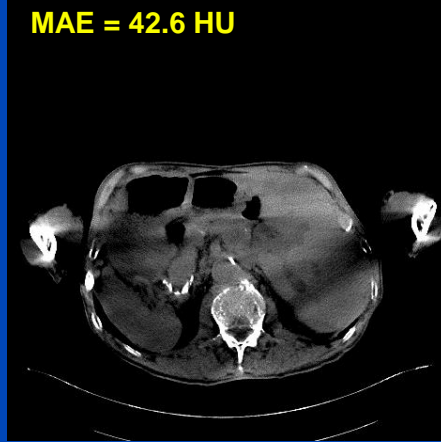
Cross-DSE

Ground Truth



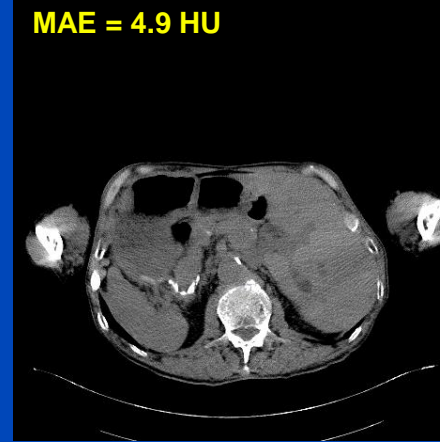
Uncorrected

MAE = 42.6 HU



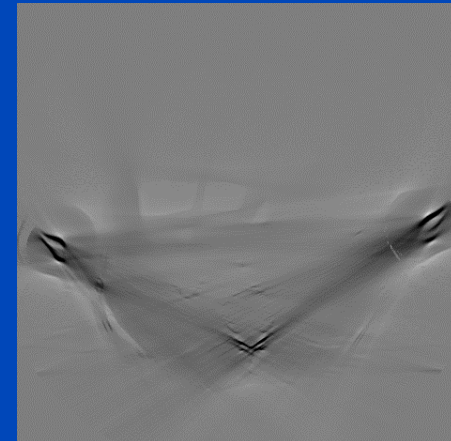
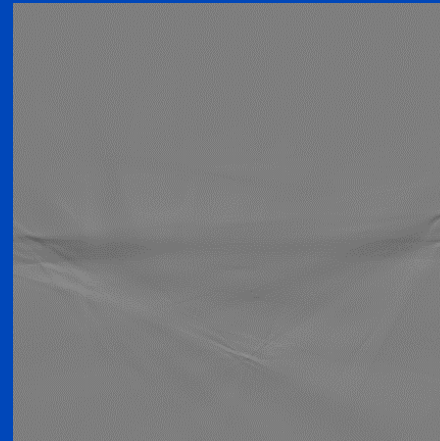
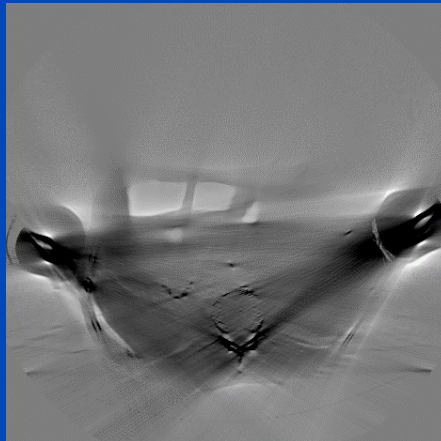
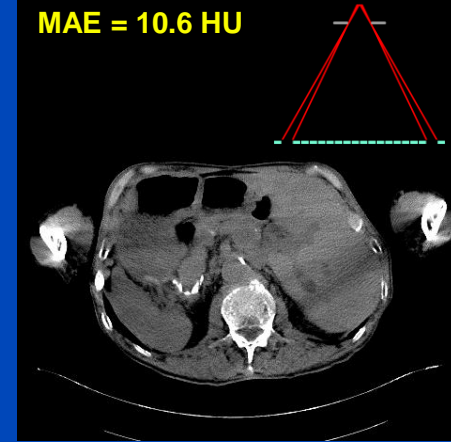
xDSE (2D, xSSE)

MAE = 4.9 HU



Measurement-based

MAE = 10.6 HU



xDSE (2D, xSSE) maps

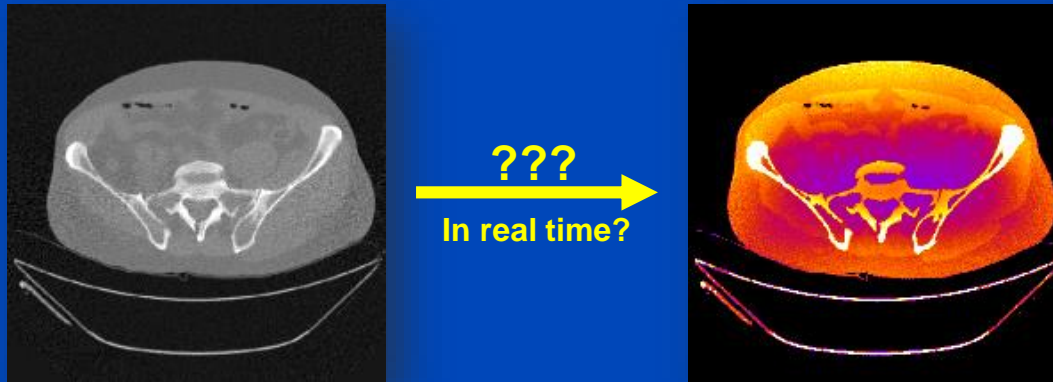
primary + forward scatter + cross-scatter + cross-scatter approximation → cross-scatter

Images $C = 40$ HU, $W = 300$ HU, difference images $C = 0$ HU, $W = 300$ HU

Conclusions on DSE

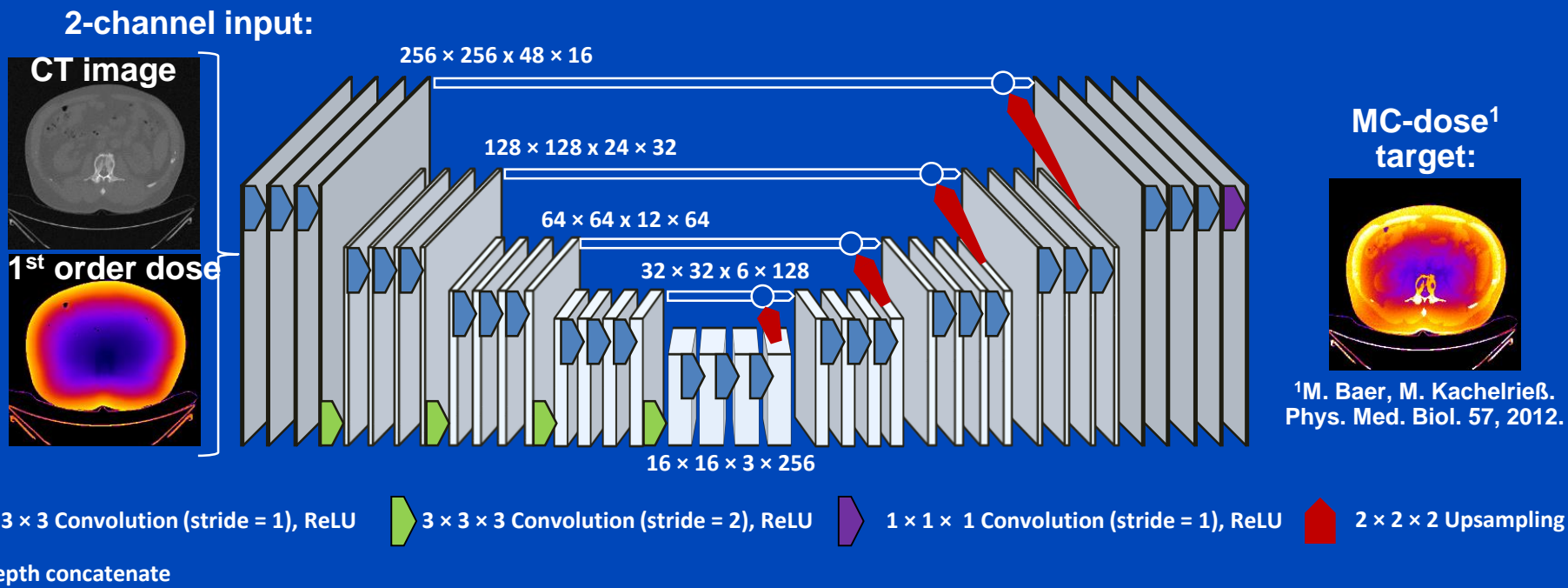
- DSE needs about 3 ms per CT and 10 ms per CBCT projection (as of 2020).
- DSE is a fast and accurate alternative to MC simulations.
- DSE outperforms kernel-based approaches in terms of accuracy and speed.
- Facts:
 - DSE can estimate scatter from a single (!) x-ray image.
 - DSE can accurately estimate scatter from a primary+scatter image.
 - DSE generalizes to all anatomical regions.
 - DSE works for geometries and beam qualities differing from training.
 - DSE may outperform MC even though DSE is trained with MC.
- DSE is not restricted to reproducing MC scatter estimates.
- DSE can rather be trained with any other scatter estimate, including those based on measurements.

Deep Dose Estimation



Deep Dose Estimation (DDE)

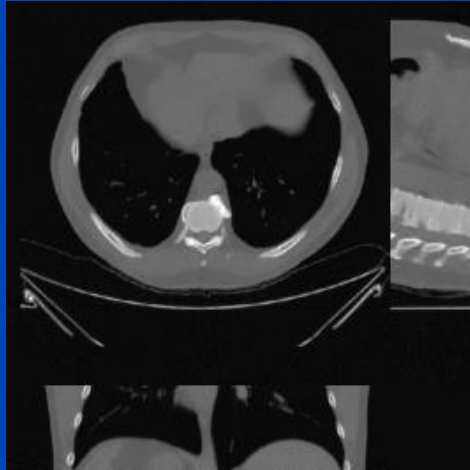
- Combine fast and accurate CT dose estimation using a deep convolutional neural network.
- Train the network to reproduce MC dose estimates given the CT image and a first-order dose estimate.



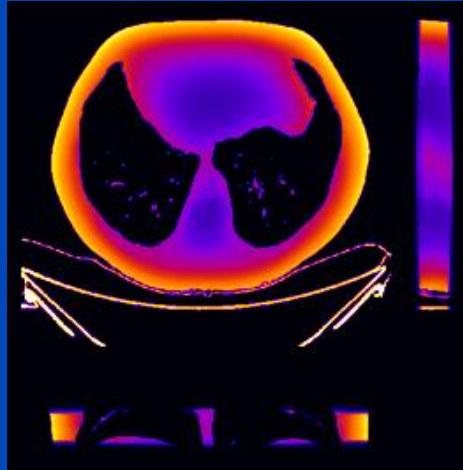
Results

Thorax, tube A, 120 kV, no bowtie

CT image



First order dose

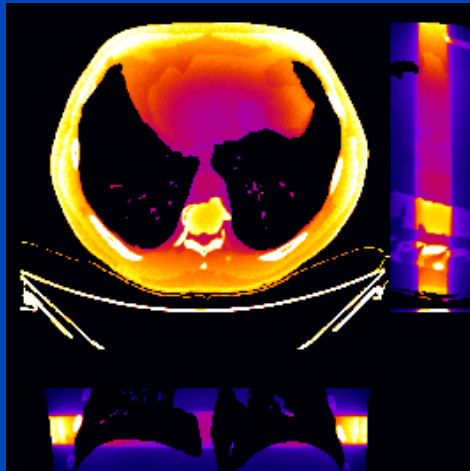


	MC	DDE
48 slices	1 h	0.25 s
whole body	20 h	5 s

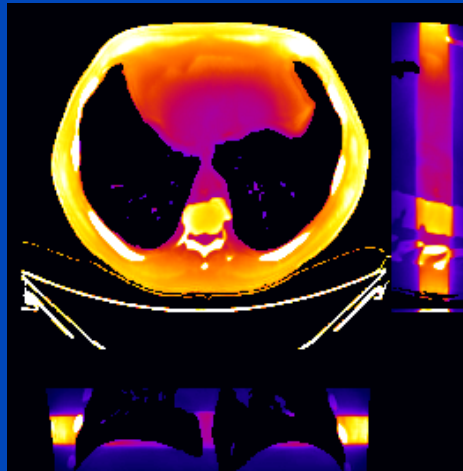
MC uses 16 CPU kernels
DDE uses one Nvidia Quadro P600 GPU

DDE training took 74 h for 300 epochs,
1440 samples, 48 slices per sample

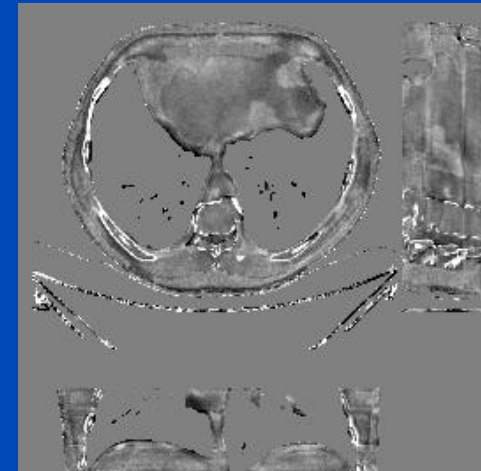
MC ground truth



DDE



Relative error



C = 0%
W = 40%

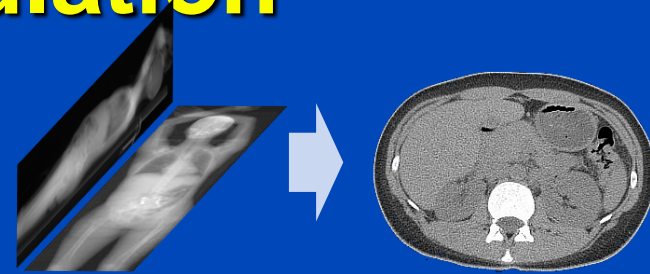
Conclusions on DDE

- **DDE provides accurate dose predictions**
 - for circle scans
 - for sequence scans
 - for partial scans (less than 360°)
 - for limited angle scans (less than 180°)
 - for spiral scans
 - for different tube voltages
 - for scans with and without bowtie filtration
 - for scans with tube current modulation
- **In practice it may therefore be not necessary to perform separate training runs for these cases.**
- **Thus, accurate real-time patient dose estimation may become feasible with DDE.**

Patient Risk-Minimizing Tube Current Modulation

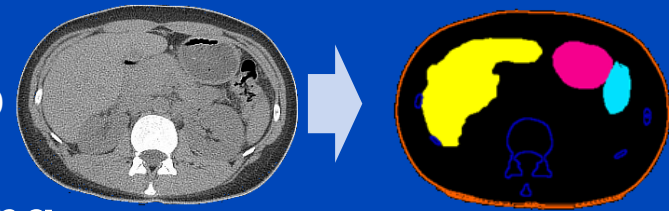
1. Coarse reconstruction from two scout views

- E.g. X. Ying, et al. X2CT-GAN: Reconstructing CT from biplanar x-rays with generative adversarial networks. CVPR 2019.



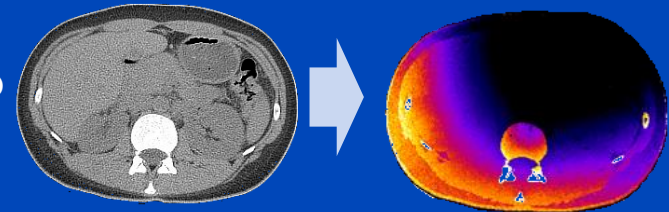
2. Segmentation of radiation-sensitive organs

- E.g. S. Chen, M. Kachelrieß et al., Automatic multi-organ segmentation in dual-energy CT (DECT) with dedicated 3D fully convolutional DECT networks. Med. Phys. 2019.



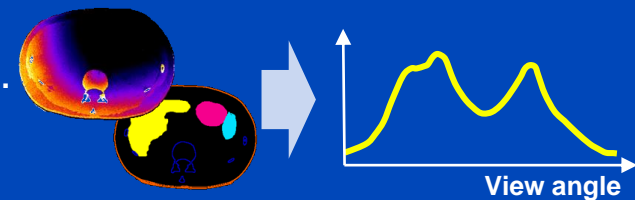
3. Calculation of the effective dose per view using the deep dose estimation (DDE)

- J. Maier, E. Eulig, S. Dorn, S. Sawall and M. Kachelrieß. Real-time patient-specific CT dose estimation using a deep convolutional neural network. IEEE Medical Imaging Conference Record, M-03-178: 3 pages, Nov. 2018.

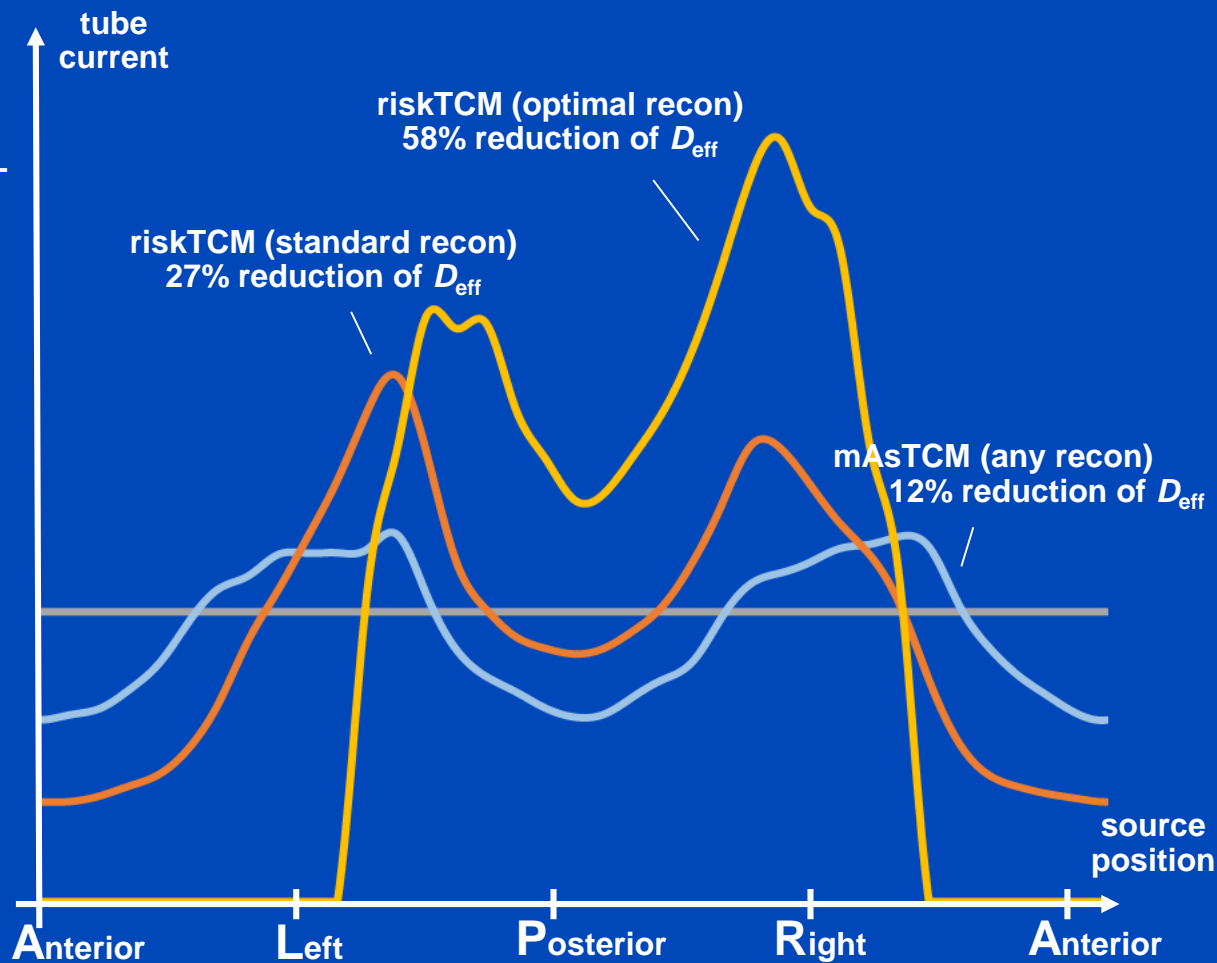
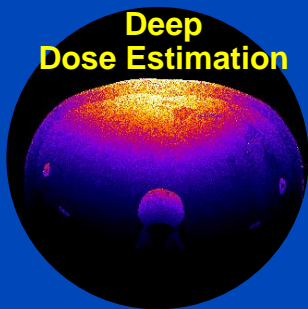
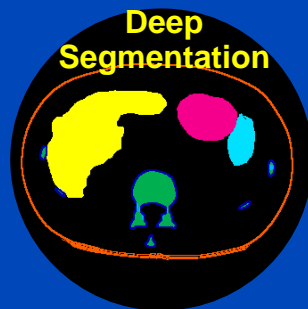
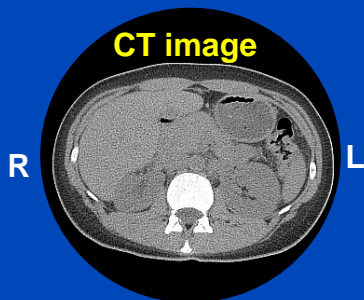


4. Determination of the tube current modulation curve that minimizes the radiation risk

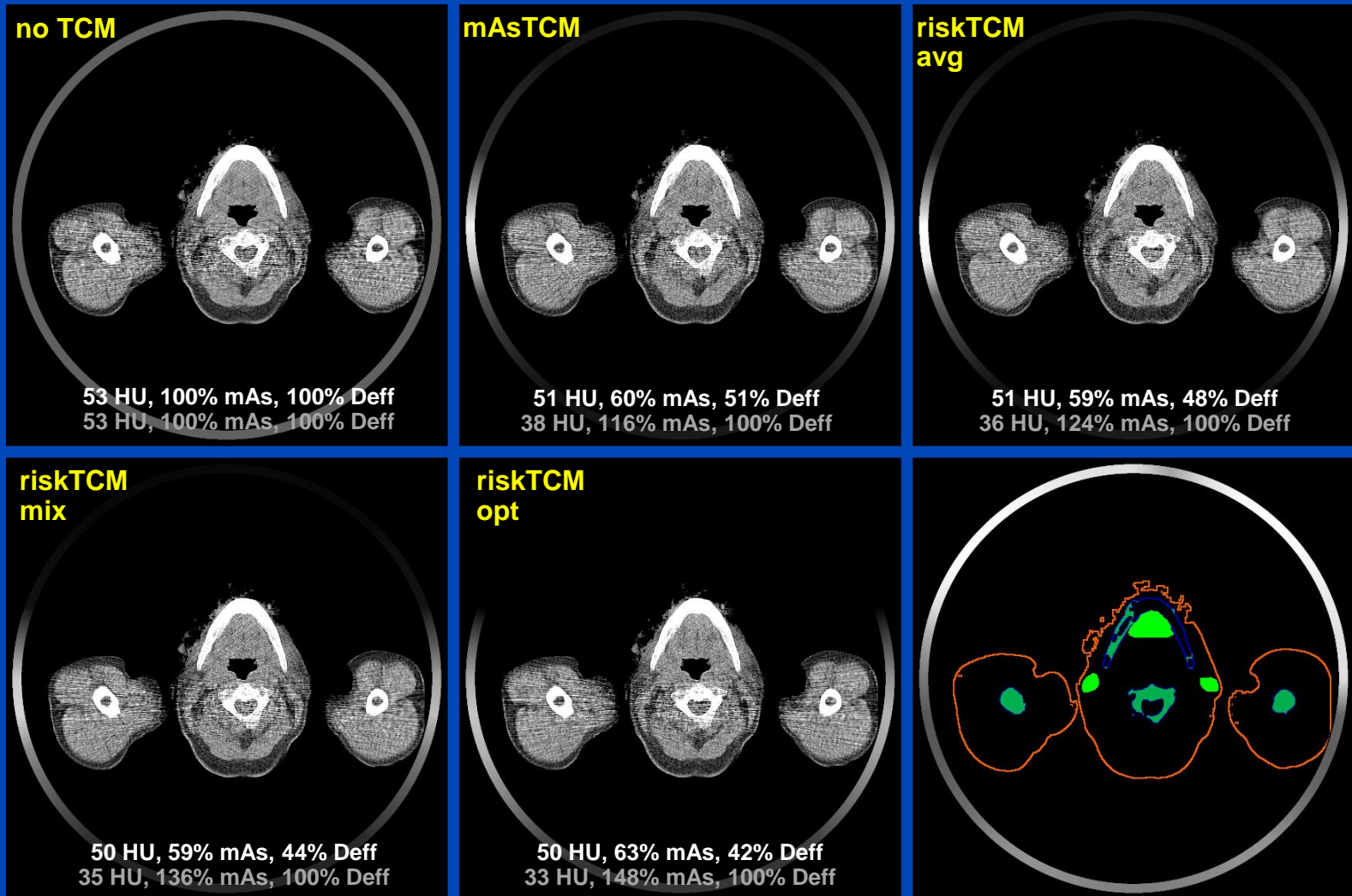
- L. Klein, J. Maier, C. Liu, A. Maier, M. Lell, and M. Kachelrieß. Patient radiation risk–minimizing tube current modulation for diagnostic CT. Submitted to Med. Phys., 2021.



Remainder 0.12
Bone surface 0.01
Brain 0.01
Breast 0.12
Colon 0.12
Red Bone Marrow 0.12
Salivary glands 0.01
Esophagus 0.04
Liver 0.04
Lung 0.12
Skin 0.01
Stomach 0.12
Gonads 0.08
Thyroid 0.04
Bladder 0.04



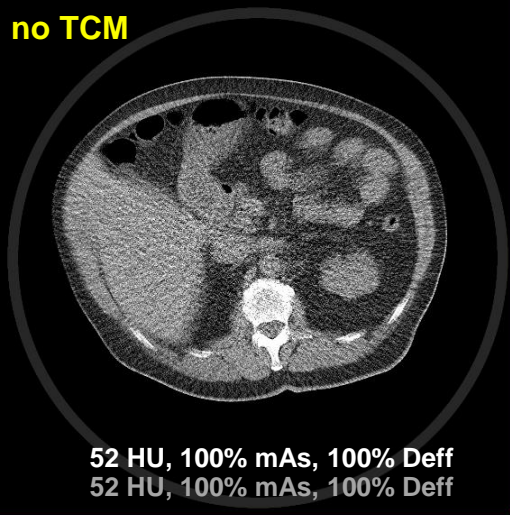
Patient 03 - Neck



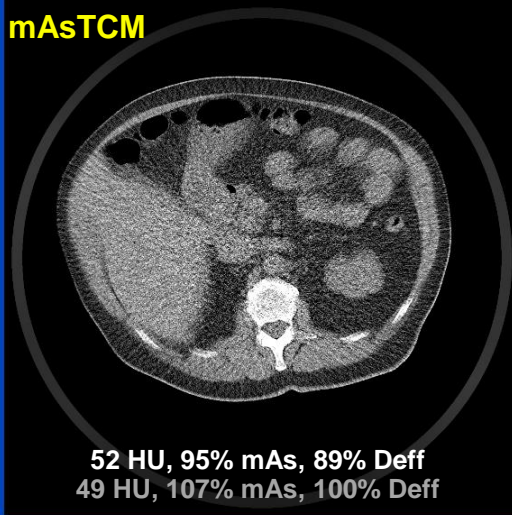
C = 25 HU, W = 400 HU

Patient 04 - Abdomen

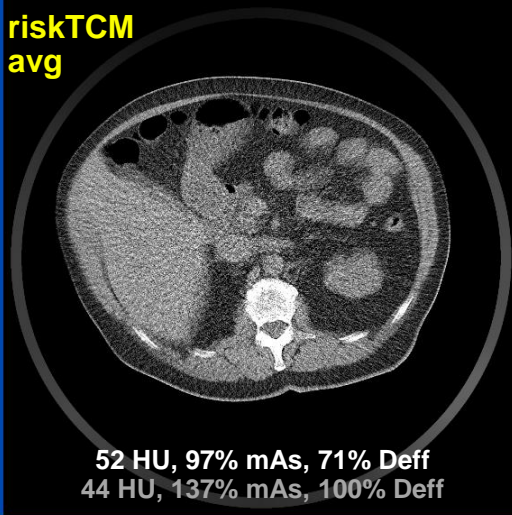
no TCM



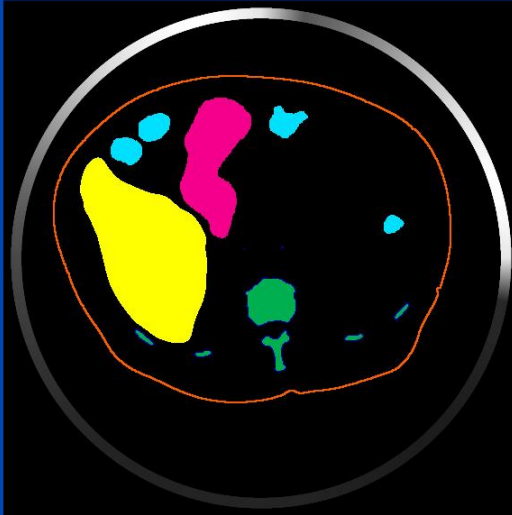
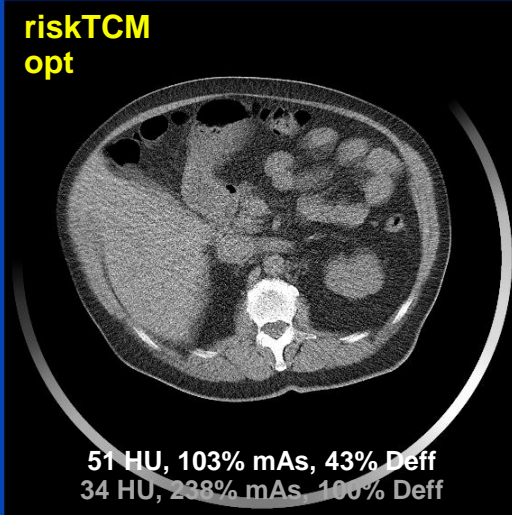
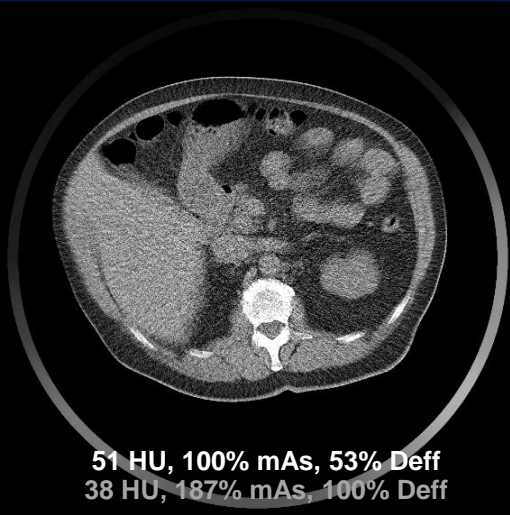
mAsTCM



riskTCM
avg



riskTCM
opt

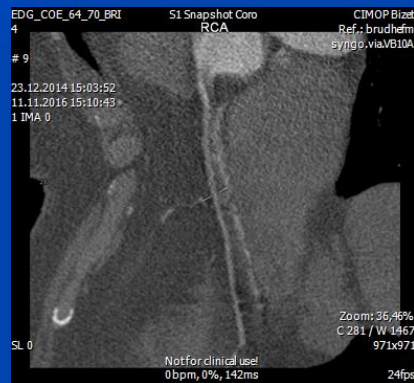


Re	0.12
BS	0.01
Br	0.01
Br	0.12
Co	0.12
RB	0.12
SG	0.01
Es	0.04
Li	0.04
Lu	0.12
Sk	0.01
St	0.12
Go	0.08
Th	0.04
BI	0.04

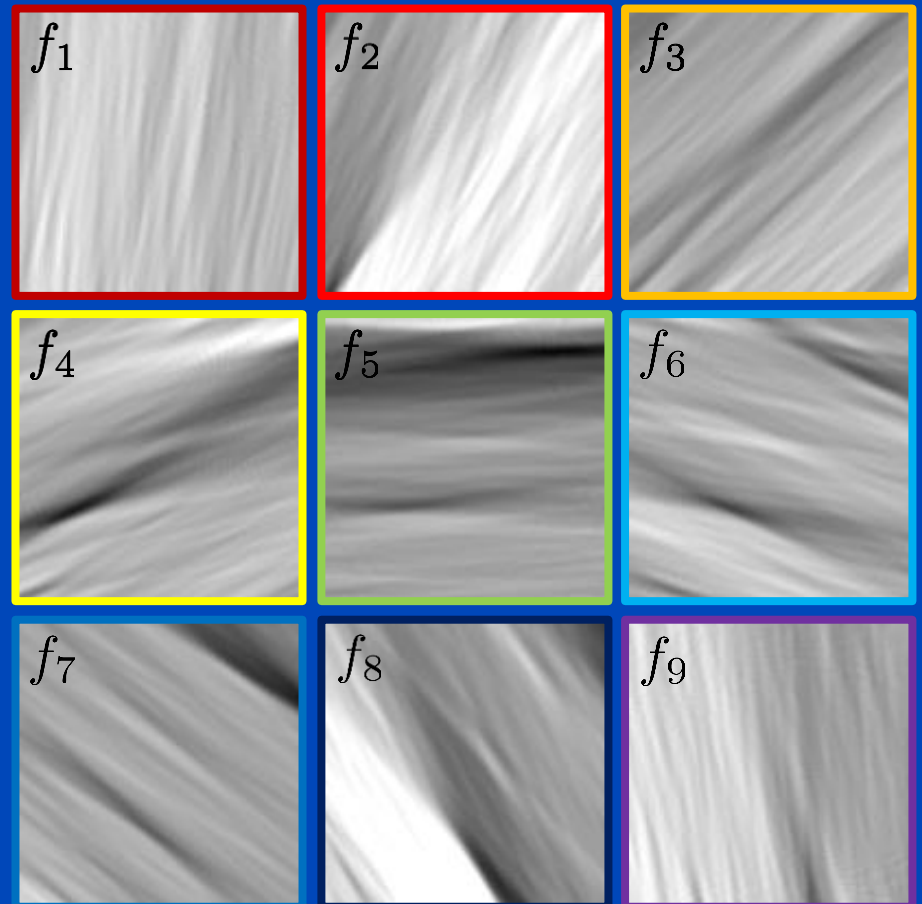
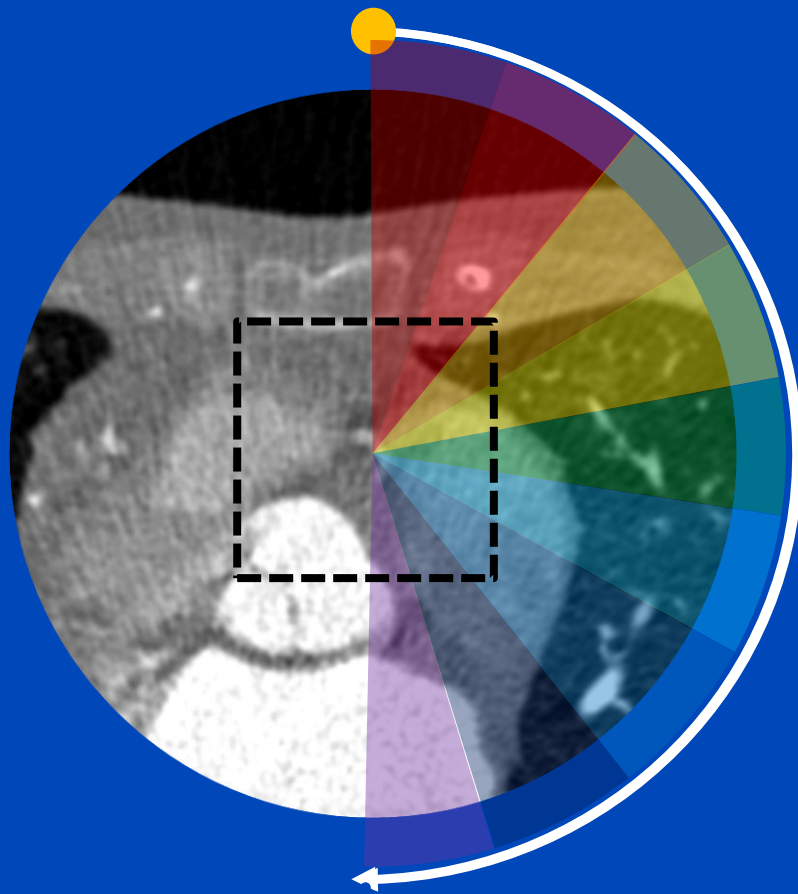
Conclusions on riskTCM

- Thanks to AI, significant risk reductions can be achieved with risk-specific tube current modulation.
- Technology-wise the method is ready to be implemented.
- Risk-specific TCM does not require hardware changes.
- It is up to the vendors to take action!

Deep Cardiac Motion Compensation

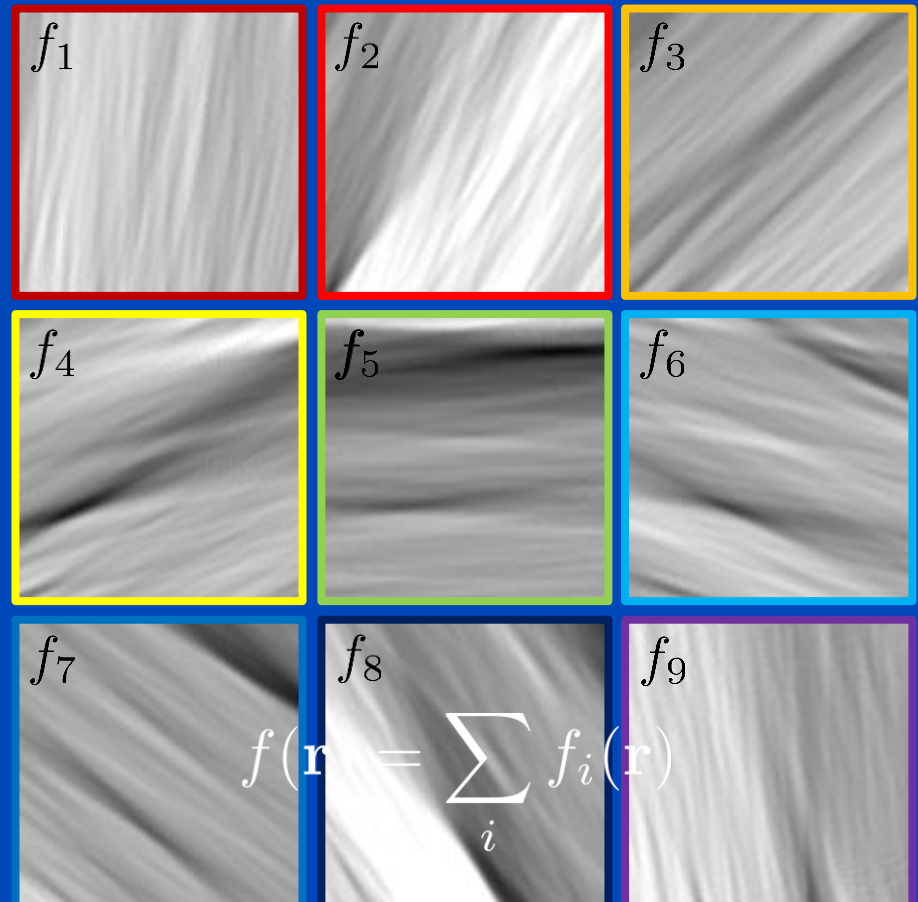
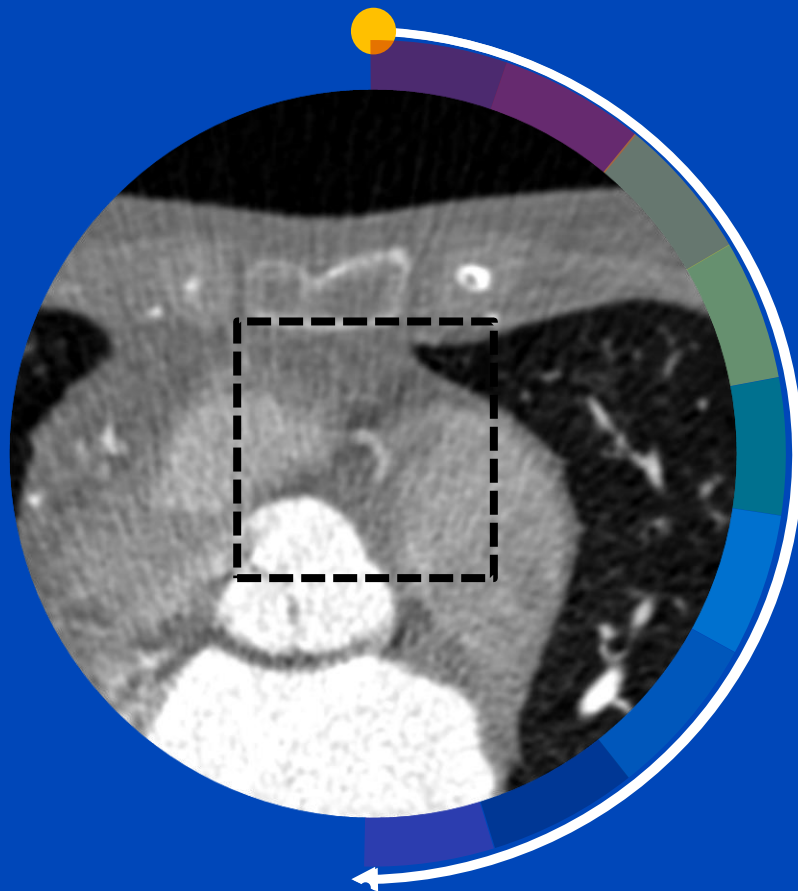


Partial Angle-Based Motion Compensation (PAMoCo)

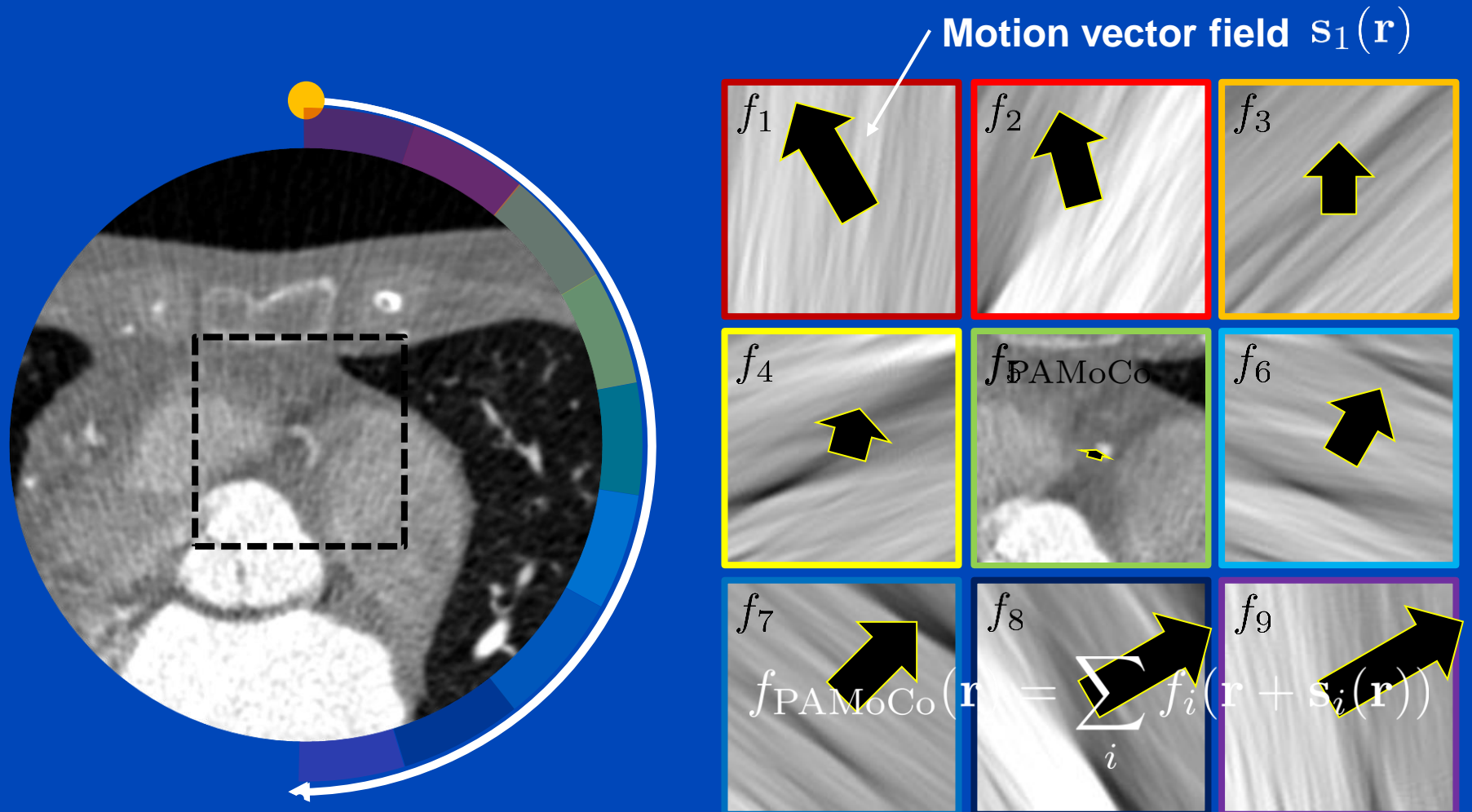


Animated rotation time = 100 × real rotation time

Partial Angle-Based Motion Compensation (PAMoCo)



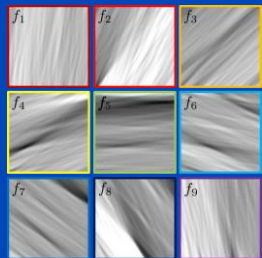
Partial Angle-Based Motion Compensation (PAMoCo)



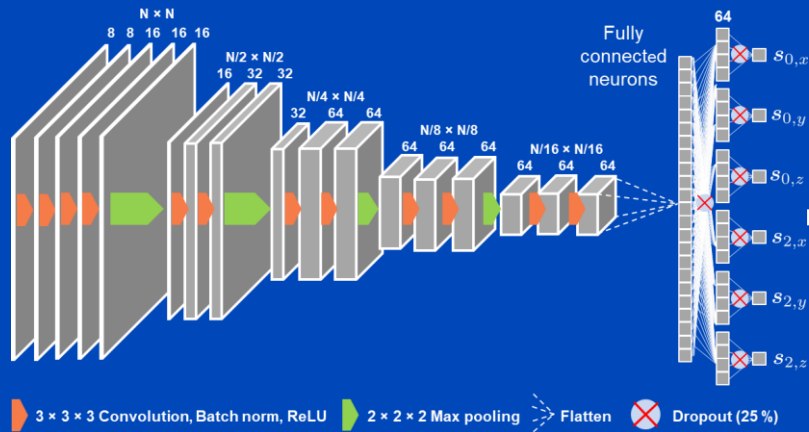
Apply motion vector fields (MVFs) to partial angle reconstructions

Deep Partial Angle-Based Motion Compensation (Deep PAMoCo)

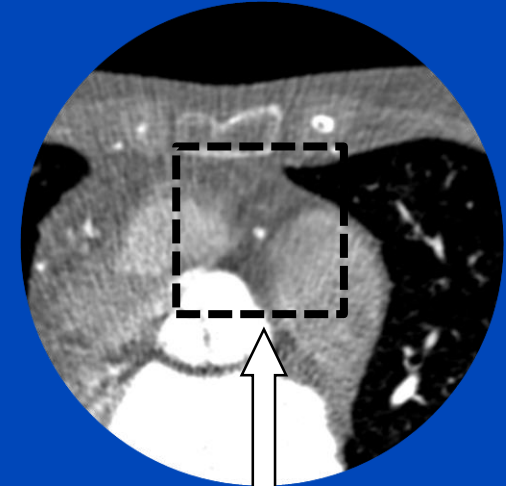
PARs centered around coronary artery



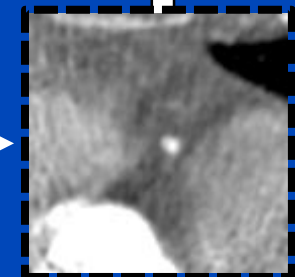
Neural network to predict parameters of a motion model



Reinsertion of patch into initial reconstruction



Spatial transformer

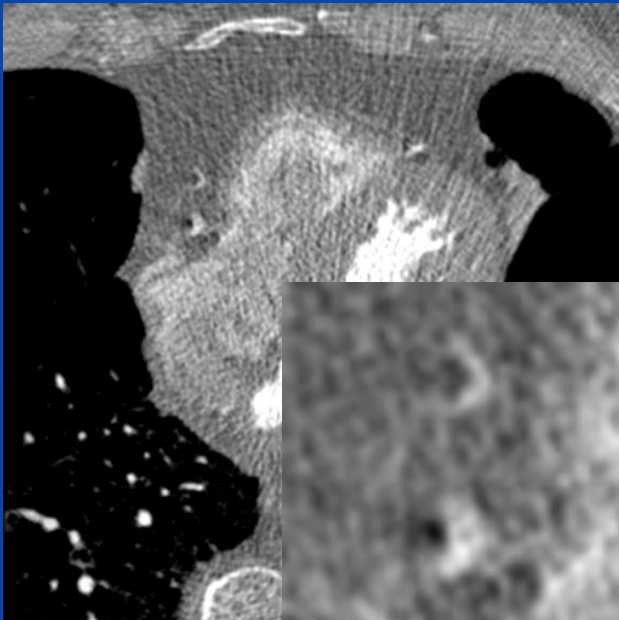


Application of the motion model to the PARs via a spatial transformer¹

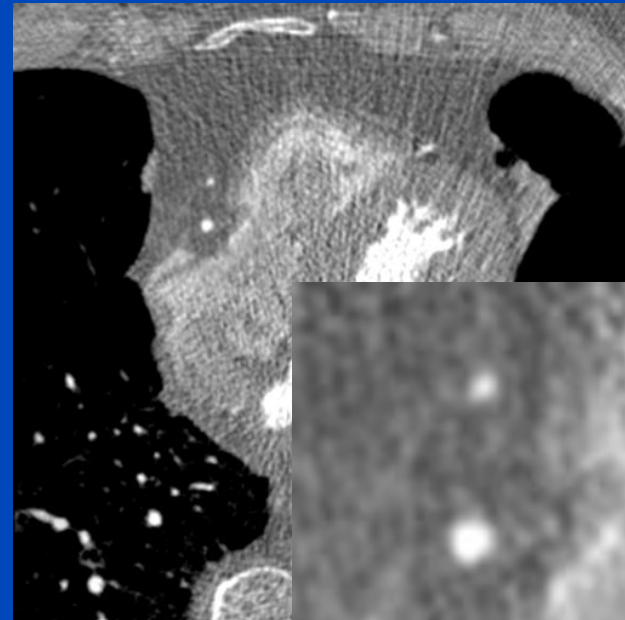
[1] M. Jaderberg et al., "Spatial transformer networks", NIPS 2015: 2017–2025 (2015).

Patient 1

Original



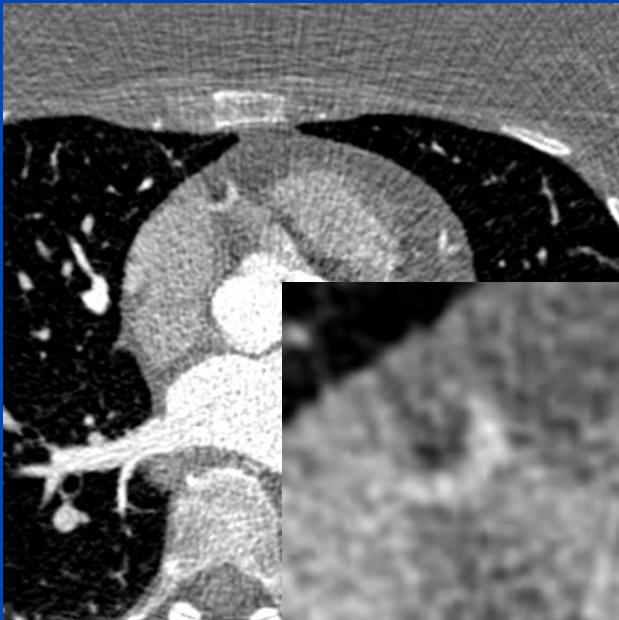
Deep PAMoCo



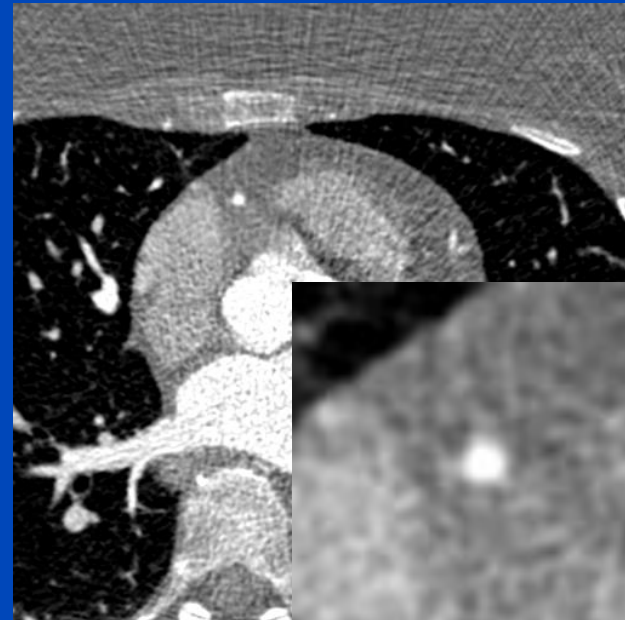
$C = 0 \text{ HU}$, $W = 1400 \text{ HU}$

Patient 2

Original



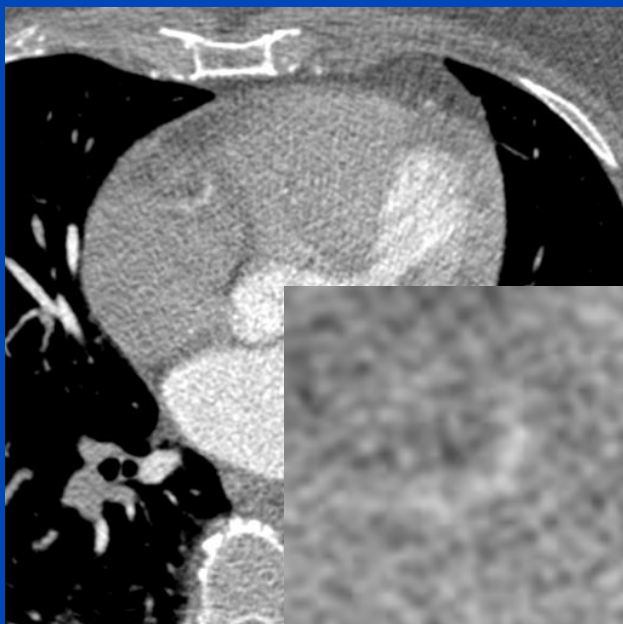
Deep PAMoCo



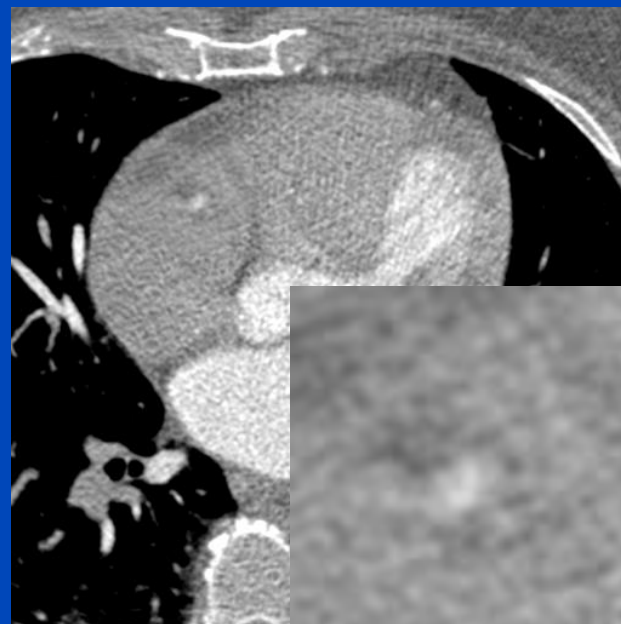
$C = 0 \text{ HU}$, $W = 1600 \text{ HU}$

Patient 3

Original



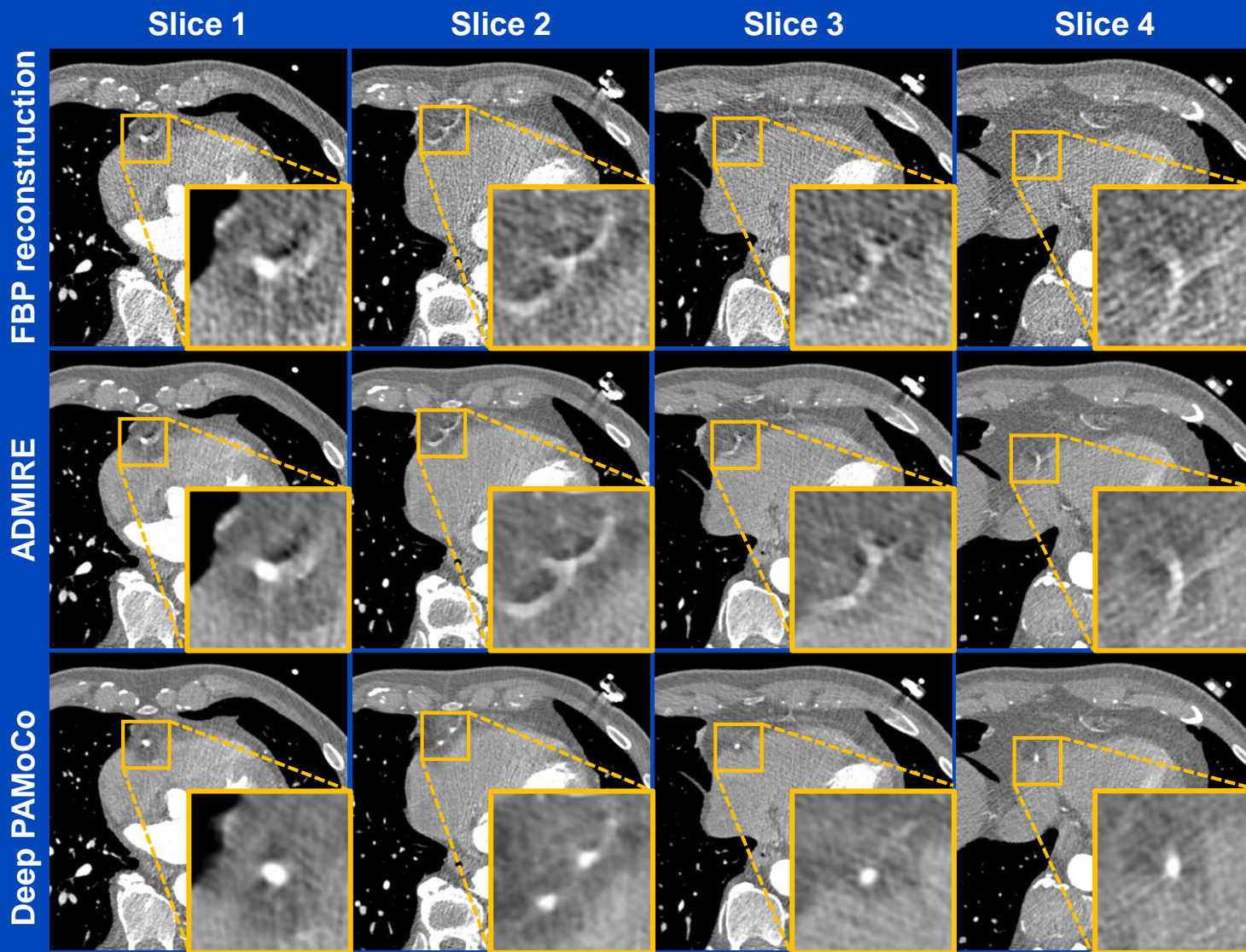
Deep PAMoCo



$C = 0 \text{ HU}$, $W = 1000 \text{ HU}$

Patient 4

Measurements at a Siemens Somatom AS



C = 0 HU, W = 1200 HU

Thank You!



This presentation will soon be available at www.dkfz.de/ct.

Job opportunities through DKFZ's international PhD or Postdoctoral Fellowship programs (marc.kachelriess@dkfz.de).

Parts of the reconstruction software were provided by RayConStruct[®] GmbH, Nürnberg, Germany.